forests

MDPI

Article

Photosynthetic Response of *Larix gmelinii* var. *japonica* Saplings After Exogenous Glutathione Foliar Application

Resa Sri Rahayu [1], Wataru Ishizuka [2], Ayu Narita [2], Rie Miyata [2], Naoko H. Miki [3], Hirokazu Kon [2] and Yuko Miyazaki [3,*]

[1] Graduate School of Environmental, Life, Natural Science and Technology, Okayama University, Okayama 700-8530, Japan; resa.rahayu@gmail.com
[2] Forestry Research Institute, Hokkaido Research Organization, Bibai 079-0198, Japan; ishizuka-wataru@hro.or.jp (W.I.); narita-ayu@hro.or.jp (A.N.); miyata-rie@hro.or.jp (R.M.); kon-hirokazu@hro.or.jp (H.K.)
[3] Faculty of Environmental, Life, Natural Science and Technology, Okayama University, Okayama 700-8530, Japan; miki@okayama-u.ac.jp
* Correspondence: yukomiyazaki@okayama-u.ac.jp

Abstract

Sapling survival and growth depend on photosynthetic assimilates. Therefore, improving physiological performance during early stages may enhance subsequent performance and nursery production. This study evaluated whether exogenous oxidized glutathione (GSSG), reported to enhance photosynthesis, improves the photosynthetic, physiological, and growth-related traits of *Larix gmelinii* var. *japonica* saplings. Sixteen saplings were assigned to four treatments: GSSG, 5-aminolevulinic acid, Hyponex, and a water control. Photosynthetic, nitrogen-related, and growth traits were measured before treatment and at 3, 6, 13, and 31 days after treatment, and biomass was assessed after three months. The GSSG treatment showed no difference in the net CO_2 assimilation rate (A_{max}) compared with the control, but exhibited a significantly earlier peak at 6 days than the other treatments. This response was supported by the stability of GSSG-treated saplings against photoinhibition (F_v/F_m) and a tendency toward greater resilience to midday light stress (Φ_{PSII}). Enhanced photosynthetic performance was associated with reduced carbon and nitrogen fluctuations and was accompanied by numerically greater root and stem biomass in the 2024 terminal shoots. Although fertilization effects were generally weak and transient, GSSG elicited notable responses, suggesting that the immediate enhancement of photosynthesis underlies its impact. However, its antioxidant properties under stressful conditions warrant further investigation.

Keywords: exogenous glutathione; foliar fertilizer; *Larix gmelinii* var. *japonica*; photosystem II quantum yield; photosynthetic rate

Check for updates

Academic Editors: Nebi Bilir, Kyu Suk Kang and Marianthi Tsakaldimi

Received: 27 March 2026
Revised: 24 April 2026
Accepted: 25 April 2026
Published: 28 April 2026

Copyright: © 2026 by the authors. Licensee MDPI, Basel, Switzerland. This article is an open access article distributed under the terms and conditions of the Creative Commons Attribution (CC BY) license.

1. Introduction

Sapling growth and survival depend on the availability of photosynthetic assimilates. In cool-temperate deciduous forests, the relative growth rate of understory seedlings increases after gap formation and is strongly correlated with the photosynthetic capacity of newly expanded leaves [1]. Leaf-level photosynthetic rates have also been positively correlated with sapling growth in temperate tree species [2]. Sapling survival in temperate tree species is closely associated with annual foliar CO_2 assimilation [3]. As growth is a key determinant of survival, the photosynthetic performance of saplings is a critical factor in

determining whether a species can establish sufficient numbers of individuals to maintain populations, particularly under changing climatic conditions [4].

Larix gmelinii var. *japonica* (Kuril larch), a regional variation of *L. gmelinii*, is found in the Sakhalin and Kuril Islands, Russia, and was also present in Hokkaido, Japan, during the last glacial period [5]. It has been crossbred with *Larix kaempferi* (Japanese larch) to create a hybrid, known as hybrid larch F1 (*L. gmelinii* var. *japonica* × *L. kaempferi*), which has desirable traits and is economically valuable [5,6]. In recent years, Japan has produced approximately 18 million larch saplings, including Kuril larch (230,000), Japanese larch (16.17 million), hybrid larch F1 (789,000), and Clean larch F1 (883,000) [7,8]. These volumes have increased over the years and are expected to increase further [7,8]. The relatively low number of *L. gmelinii* var. *japonica* saplings is thought to result from growth inhibition relative to other *Larix* species [9–12] and from the fact that its sapling production is limited to Hokkaido, Japan. To meet target production volumes, the sustainability of *L. gmelinii* var. *japonica* saplings should be considered. Moreover, *Larix* saplings show low survival and growth, both in the nursery, due to nursery practices [5,13] and after planting under various intensities of competition [6,14], similar to other conifer species [15].

Because seeds of the genus *Larix* generally have a low germination rate [16–19] and cannot produce enough seedlings to meet the demand for nursery stock [5], propagation of *Larix* is typically carried out vegetatively, that is, through rooted cuttings [5]. The need for efficient production has led to a shift from traditional nurseries to in-house, container-based *Larix* production systems. This change not only improves efficiency but also has the advantage that container-grown seedlings exhibit better growth and survival after planting [13,14]. As noted above, sapling growth and survival are influenced by the availability of photosynthetic assimilates. Therefore, increasing the photosynthetic capacity of *L. gmelinii* var. *japonica* saplings is expected to enhance production, thereby helping to meet the demand for increased larch production in Japan.

The enhancement of photosynthetic efficiency as a means of improving productivity has been extensively studied in various crop species [20]. However, the direct manipulation of photosynthesis in woody plants, particularly conifers, remains limited because of their long life cycles and complex source–sink relationships. Consequently, alternative approaches that indirectly influence physiological performance may provide practical options for improving the seedling growth of forest tree species. Glutathione, an essential metabolite with multiple functions in plants, is involved in various developmental processes, including biosynthetic pathways, detoxification, antioxidant biochemistry, and redox homeostasis [20]. Previous research has shown that glutathione enhances photosynthesis to alleviate stress by mitigating oxidative stress in some plant species, including annual grasses [21–23] and annual herbs [24–29]. However, the detailed mechanisms underlying this increase in photosynthesis remain unclear. Moreover, there is no information regarding this issue in woody plants, especially conifers. Therefore, this study aimed to evaluate whether exogenous oxidized glutathione improves the photosynthetic, physiological, and growth-related traits of *L. gmelinii* var. *japonica* saplings and to examine the associated physiological responses.

2. Materials and Methods

2.1. Plant Materials

Three-year-old *Larix gmelinii* var. *japonica* saplings obtained from the Forest Research Institute (Bibai, Hokkaido, Japan) were used in this study. Saplings were individually planted in plastic pots (5 cm in diameter and 15 cm in height) filled with a 1:1 (*v*/*v*) mixture of vermiculite and akadama soil (aggregate-like soil, 2–6 mm in diameter). This mixed medium was an inorganic growing medium; therefore, the nutrients for the saplings

were supplied solely by fertilization. The saplings were fertilized with a liquid fertilizer (Hyponex; N–P–K composition: 6–10–5; HYPONeX, Osaka, Japan) at a concentration of 1 mL L^{-1} once every two weeks and watered daily. All saplings were grown in a nursery at Okayama University (34.686, 133.916; Tsushima Campus, Okayama, Japan) under a fiber-roofed structure to prevent direct rainfall and sunlight under ambient environmental conditions. At the start of the experiment (May 2024), these three-year-old saplings had a mean height of 59.9 ± 8.9 cm and a mean stem diameter of 0.83 ± 0.04 cm. The experiment was conducted from May to August 2024 under natural photoperiodic conditions.

2.2. Foliar Spray Treatment

Sixteen *L. gmelinii* var. *japonica* saplings were assigned to four foliar spray treatments (n = 4 per treatment): (1) oxidized glutathione (GSSG; 1000× dilution of Kaneka Peptide W2, containing 0.1 g L^{-1} oxidized glutathione; Kaneka, Osaka, Japan), (2) 5-aminolevulinic acid (ALA; 1000× dilution of ALA-FeSTA; SAKATA SEED, Yokohama, Japan), (3) a commercial fertilizer (Hyponex Professional; N–P–K = 20–20–20; 500× dilution; HYPONeX, Osaka, Japan), and (4) tap water as a control. Kaneka Peptide W2 and ALA-FeSTA contain pre-added N, P, and K. By establishing an NPK treatment with the same nitrogen concentration (0.125 g L^{-1}) as the GSSG and ALA treatment solutions, we evaluated the effects of oxidized glutathione and 5-aminolevulinic acid (Table 1) [30–32]. Each treatment solution was applied once via foliar spraying in early July 2024. Approximately 0.5 L of solution was applied to each sapling, ensuring complete coverage. To avoid cross-contamination, the treatments were applied separately, with added spacing between samples. Foliar spraying was performed in the morning, after which the saplings were maintained in a shaded area to avoid direct sunlight.

Table 1. Establishment of NPK treatment with the same nitrogen concentration as GSSG and ALA treatment solutions.

Fertilizer Concentrations					
Process	**Kaneka Peptide W2 (10-10-10)**	**ALA-FeSTA (4.5-6.5-5.5)**	**Professional Hyponex (20-20-20)**		
NPK+ALA	1000 times	1000 times	2500 times		
NPK+GSSG			8000 times		
NPK			1600 times		
Content (g L^{-1}) [1]					
Process	**GSSG**	**ALA**	**N**	**P**	**K**
NPK+ALA	0.1	Not clear	0.125	0.145	0.135
NPK+GSSG			0.125	0.125	0.125
NPK			0.125	0.125	0.125
Weighing of fertilizer (g) for 0.5 L solution [2]					
Process	**Kaneka Peptide W2 (10-10-10)**	**ALA-FeSTA (4.5-6.5-5.5)**	**Professional Hyponex (20-20-20)**		
NPK+ALA	0.5	0.5	0.2		
NPK+GSSG			0.0625		
NPK			0.3125		

[1] Content = Mixture ratio × 1000 g (=1 L)/(dilution ratio). [2] Weight (g) = volume of water (mL)/dilution ratio; for ALA-FeSTA only, mL.

2.3. Repeated Measurements

Repeated measurements were conducted 2 d before treatment (day 0, pretreatment) and 3, 6, 13, and 31 d after treatment to assess photosynthetic, nitrogen-related, and growth traits. Measurements were performed on all saplings on each observation day.

2.4. Gas-Exchange Measurements

The light-saturated net photosynthetic rate (A_{max}) was measured using an LI-6400/XT Portable Photosynthesis System (LI-COR, Lincoln, NE, USA) equipped with a 6 cm^2 leaf chamber. For each measurement, seven fully expanded current-year needles located in the upper position were gently aligned with their adaxial surfaces facing upward, fixed using tape, and placed together in the leaf chamber to ensure sufficient leaf area coverage. Photosynthetically active radiation was set at 1600 µmol photons m^{-2} s^{-1} to achieve light-saturated conditions.

Measurements were conducted under controlled conditions with a leaf chamber at a temperature of 25 °C and a relative humidity of approximately 70%. The reference CO_2 concentration was maintained at 370 ppm with a flow rate of 500 µmol s^{-1}. The measurements were performed from morning to noon. For each sapling, gas exchange measurements were performed three times using different sets of needles. After each measurement, seven needles were collected, and the total projected leaf area was determined using ImageJ software (v.1.54i; National Institutes of Health, Bethesda, MD, USA) [33]. The area-based A_{max} (µmol CO_2 m^{-2} s^{-1}) was calculated by correcting the measured values according to the actual needle area within the chamber.

2.5. Photosystem II Quantum Yields

Photosystem II (PSII) chlorophyll fluorescence was measured using a MINI-PAM-II Photosynthesis Yield Analyzer (WALZ, Effeltrich, Germany) equipped with a modified leaf clip. For each measurement, one fully expanded current-year needle located at the upper position was selected with the adaxial surface oriented upward. The same needle was used for repeated measurements. Data were obtained via data transfer using WinControl-3 software (WALZ, Effeltrich, Germany). Measurements were conducted under field conditions at three time points: before sunrise (02:00) to obtain the minimum fluorescence yield after dark adaptation (F_0) and the maximum fluorescence yield after dark adaptation (F_m) under weak measurement light; and at midday (12:00) and in the afternoon (17:00) to obtain steady-state fluorescence under ambient light (F) and the maximum fluorescence during a saturating pulse (F'_m). Measurements were replicated five times for each sapling, resulting in 20 observational units per treatment.

Photosystem II (PSII) parameters were calculated following the saturation pulse method [34], including the effective quantum yield of PSII (Φ_{PSII}), the maximum quantum yield of PSII (F_v/F_m), and non-photochemical quenching (NPQ), defined as follows:

$$\Phi_{PSII} = \frac{(F'_m - F)}{F'_m}$$

$$F_v/F_m = \frac{(F_m - F_0)}{F_m}$$

$$\mathrm{NPQ} = \frac{(F_m - F'_m)}{F'_m}$$

2.6. Plant Height and Stem Diameter

Plant height was measured from the surface of the growth medium to the apical bud using a ruler, and stem diameter was measured approximately 1 cm above the growth medium using a vernier caliper.

2.7. Nitrogen and Carbon Analysis

The needles used for photosynthetic rate measurements (seven needles per measurement) were collected for nitrogen and carbon analyses. Needle samples were stored in

2 mL inner-lined stainless-steel microtubes at −26 °C and freeze-dried for 24 h using a freeze dryer (FDV-2110; EYELA, Tokyo, Japan). The freeze-dried needles were ground in the same microtubes using a TissueLyser II (QIAGEN, Hilden, Germany). A total of 1.50 ± 0.10 mg of ground material was weighed into 157 µL universal soft tin capsules (Thermo Fisher Scientific, Waltham, MA, USA) for analysis. Carbon and nitrogen concentrations were determined using an isotope ratio mass spectrometer (Delta V Advantage; Thermo Fisher Scientific, Waltham, MA, USA), and the C:N ratio was calculated based on the resulting mass percentages.

2.8. Leaf Mass per Area (LMA)

The needles used for the nutrient analysis were weighed after freeze-drying. Leaf mass per unit area (LMA) was calculated using the dry mass of needles and the corresponding leaf area measured during photosynthesis. LMA was expressed as dry mass per unit leaf area (g m^{-2}).

2.9. Photosynthetic Nitrogen Use Efficiency (PNUE)

Photosynthetic nitrogen use efficiency (PNUE) was calculated as the ratio of the light-saturated net photosynthetic rate (A_{max}) to leaf nitrogen content, expressed as:

$$\text{PNUE} = \frac{Amax}{(\text{LMA} \times \text{leaf nitrogen concentration})}$$

where A_{max} is given in µmol CO_2 m^{-2} s^{-1}, LMA in g m^{-2}, and leaf nitrogen concentration as a percentage of dry mass.

2.10. One-Time Measurements

2.10.1. The Terminal Shoot in 2024

Terminal shoot length in 2024 was determined by measuring the length from the most recent bud scar formed in spring to the apical bud in early autumn.

2.10.2. Dry Biomass

In early autumn of 2024, at the end of the 2024 growing season, each sapling was harvested and separated into roots, stems, and needles. The samples were oven-dried at 70 °C for 30 h and weighed to determine dry biomass. In addition, the dry masses of the 2024 annual growth and those of the 2024 needles were quantified separately.

2.10.3. Tree Ring

The width of the annual ring in 2024 was measured concurrently with biomass sampling. A stem segment of approximately 1 cm in length was excised from the basal part of each sapling. Cross-sections were observed and imaged under a stereomicroscope (Olympus SZX7; Olympus, Tokyo, Japan) at 1.6× magnification. The width of the outermost (2024) annual ring was measured from digital images using ImageJ software (v.1.54i; National Institutes of Health, Bethesda, MD, USA) [33].

2.11. Statistical Analysis

All statistical analyses and boxplot illustrations were performed using R software (version 4.4.1; R Foundation for Statistical Computing, Vienna, Austria) in RStudio (version 2024.09.0+375; Posit Software, PBC, Boston, MA, USA) [35]. Statistical analyses were performed using linear mixed-effects models (LMMs) to evaluate the influence of the fertilizer and observation time on A_{max} and all other parameters (photosynthetic, nitrogen-related, and growth traits) as response variables. Fertilizer, day, and their interaction were

included as fixed effects, and individual plants were included as random effects to account for repeated measures. The significance of fixed effects was assessed using ANOVA (F-tests) on linear mixed-effects models with Satterthwaite's approximation of degrees of freedom. Following a significant LMM result ($p < 0.05$), pairwise comparisons among treatment and observation-time groups were conducted using Tukey's post hoc tests based on estimated marginal means. Linear mixed-effects models were fitted using the lme4 package, and post hoc comparisons were conducted using the emmeans package in R (version 4.4.1; R Foundation for Statistical Computing, Vienna, Austria).

3. Results

3.1. Bud Opening and Leaf Flushing

Leaf flushing of the 2024 needles began in March, and some saplings flushed earlier than others (Figure 1). By early April 2024, all saplings had fully expanded needles and no further leaf expansion was observed. Therefore, all needles used for the foliar fertilizer treatment in early July 2024 were fully expanded and mature.

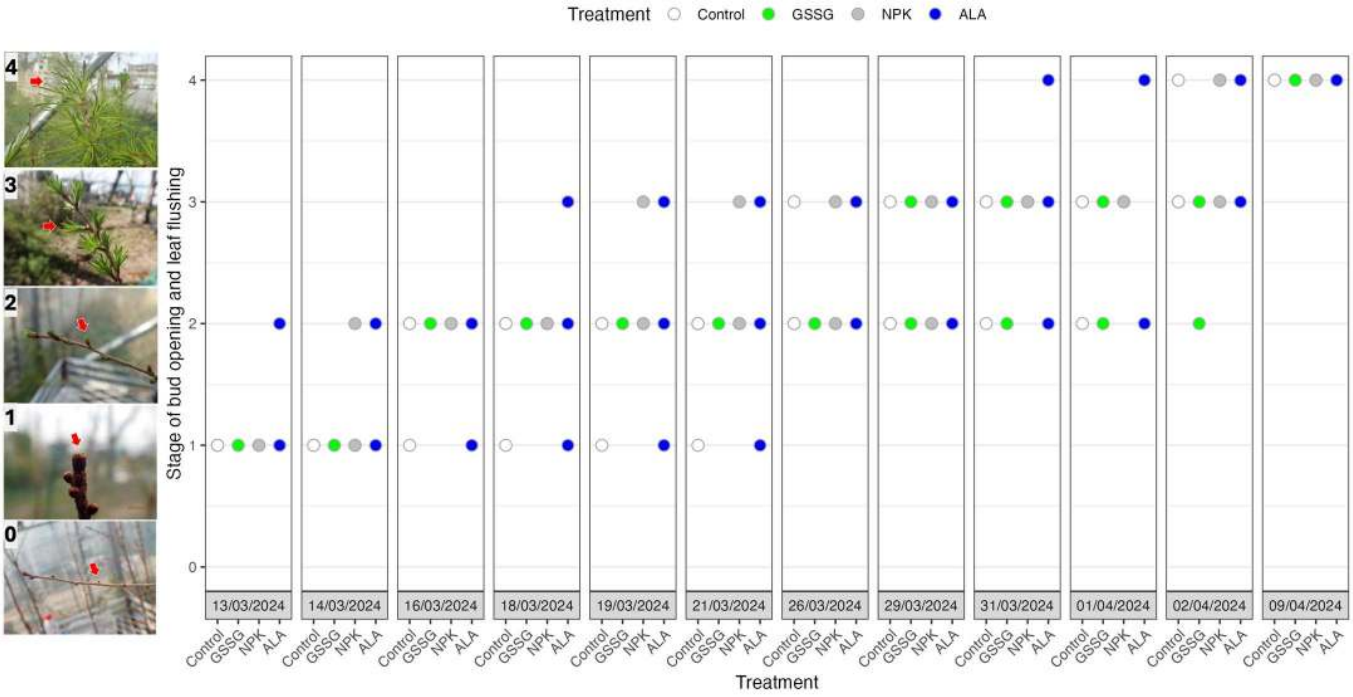

Figure 1. Stages of bud opening and leaf flushing in potted saplings of *Larix gmelinii* var. *japonica* before treatment. Stage 0 = unopened bud (brown); Stage 1 = bud opening, with green visible in the center; Stage 2 = leaf emergence (green leaves visible); Stage 3 = leaf elongation; Stage 4 = fully expanded leaves.

3.2. Photosynthetic Traits

The linear mixed-effects model revealed a significant effect of observation time on the net CO_2 assimilation rate at light saturation (A_{max}) (Table 2). No significant interactions were found between fertilizer treatment and observation time, suggesting that most treatments followed the general temporal trend of the control (Table 2). However, post hoc pairwise comparisons identified distinct temporal patterns within specific treatments (Figure 2a, Table S21). In the GSSG-fertilized group, A_{max} increased significantly 6 d after foliar application, reaching its peak earlier than in the other treatments (Figure 2a). However, it subsequently declined and returned to pretreatment levels 31 days after application (Figure 2a). In addition, no significant differences in A_{max} were detected among treatments at any observation time

point (Table S9). The other fertilization treatments and the control showed no consistent temporal changes in A_{max} over the 31-day observation period (Figure 2a).

Table 2. Linear mixed-effects model results for the effects of fertilizer treatment and observation time (Day) on the maximum photosynthetic rate (A_{max}) at light saturation. A_{max} was modeled with Fertilizer and Day as fixed factors and Plant_No as a random effect. p-values were calculated using Satterthwaite's method. The intercept represents the baseline group (Control Fertilizer at Day 0). Asterisks indicate significance: *** $p < 0.001$, * $p < 0.05$.

Term	Estimate (β)	Std. Error	df	t Value	p Value	Sig
Fixed effects						
(Intercept)	3.54732	0.64178	33.04406	5.527	0.00000387	***
Fertilizer Main Effects						
Fertilizer (GSSG)	0.22692	0.90761	33.04406	0.25	0.8041	
Fertilizer (NPK)	−0.2311	0.90761	33.04406	−0.255	0.8006	
Fertilizer (ALA)	0.60261	0.90761	33.04406	0.664	0.5113	
Day Main Effects						
Day 3	1.74297	0.67212	48	2.593	0.0126	*
Day 6	1.35976	0.67212	48	2.023	0.0487	*
Day 13	3.42188	0.67212	48	5.091	0.00000591	***
Day 31	0.15823	0.67212	48	0.235	0.8149	
Interactions: Fertilizer × Day 3						
GSSG × Day 3	−1.5018	0.95052	48	−1.58	0.1207	
NPK × Day 3	−0.47635	0.95052	48	−0.501	0.6186	
ALA × Day 3	−1.26896	0.95052	48	−1.335	0.1882	
Interactions: Fertilizer × Day 6						
GSSG × Day 6	0.77006	0.95052	48	0.81	0.4219	
NPK × Day 6	0.8822	0.95052	48	0.928	0.358	
ALA × Day 6	−1.03883	0.95052	48	−1.093	0.2799	
Interactions: Fertilizer × Day 13						
GSSG × Day 13	−2.32565	0.95052	48	−2.447	0.0181	*
NPK × Day 13	−0.31335	0.95052	48	−0.33	0.7431	
ALA × Day 13	−1.3957	0.95052	48	−1.468	0.1485	
Interactions: Fertilizer × Day 31						
GSSG × Day 31	−0.09177	0.95052	48	−0.097	0.9235	
NPK × Day 31	0.7359	0.95052	48	0.774	0.4426	
ALA × Day 31	−0.31443	0.95052	48	−0.331	0.7422	
Random effects						
Groups Name	**Variance**	**Std. Dev.**				
Plant_No (Intercept)	0.744	0.8626				
Residual	0.9035	0.9505				

Regarding photosystem II (PSII) chlorophyll fluorescence, none of the parameters were significantly affected by GSSG or any other fertilizer treatment at any observation time (Figure 2b,d–f, Tables S1–S3, S11–S13, S22–S24). However, the maximum quantum yield (F_v/F_m) indicated notable numerical trends in the GSSG treatment (Table 3), and the effective quantum yield of PSII (Φ_{PSII}) measured at midday in GSSG-treated saplings showed a significantly different value compared to the control (Figure 2c). In the GSSG-treated saplings, the F_v/F_m median values remained stable within the range of 0.785–0.805 throughout the study period (Figure 2b). Although the linear mixed-effects model revealed a significant interaction between GSSG treatment and day on Days 3 and 6 (p = 0.007 and 0.019) (Table 4), post hoc analysis indicated no significant temporal variations in F_v/F_m within treatments (Figure 2b), and there were no significant differences between treatments at any observation time point (Table 5). Numerical trends indicated that F_v/F_m in GSSG-treated saplings remained stable from Day 0 to Day 31; the estimated change was nearly zero (−0.003, p = 0.998), suggesting that overall levels returned to the baseline or did not deviate significantly from Day 0 (Table 3). Furthermore, the GSSG treatment

showed a notable upward trend in F_v/F_m following the initial period, with a near-significant improvement observed between Days 3 and 13 (t = 2.74, p = 0.065) (Table 3).

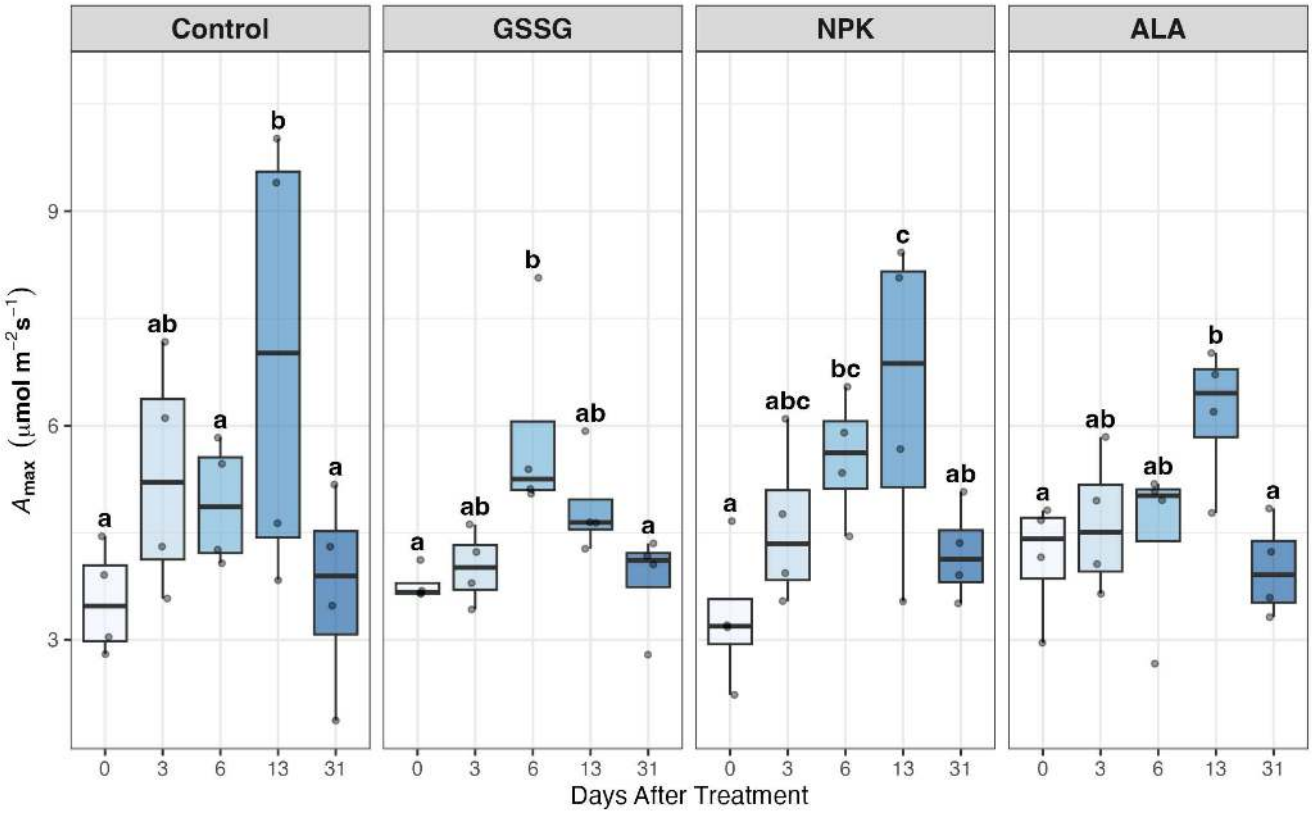

(a)

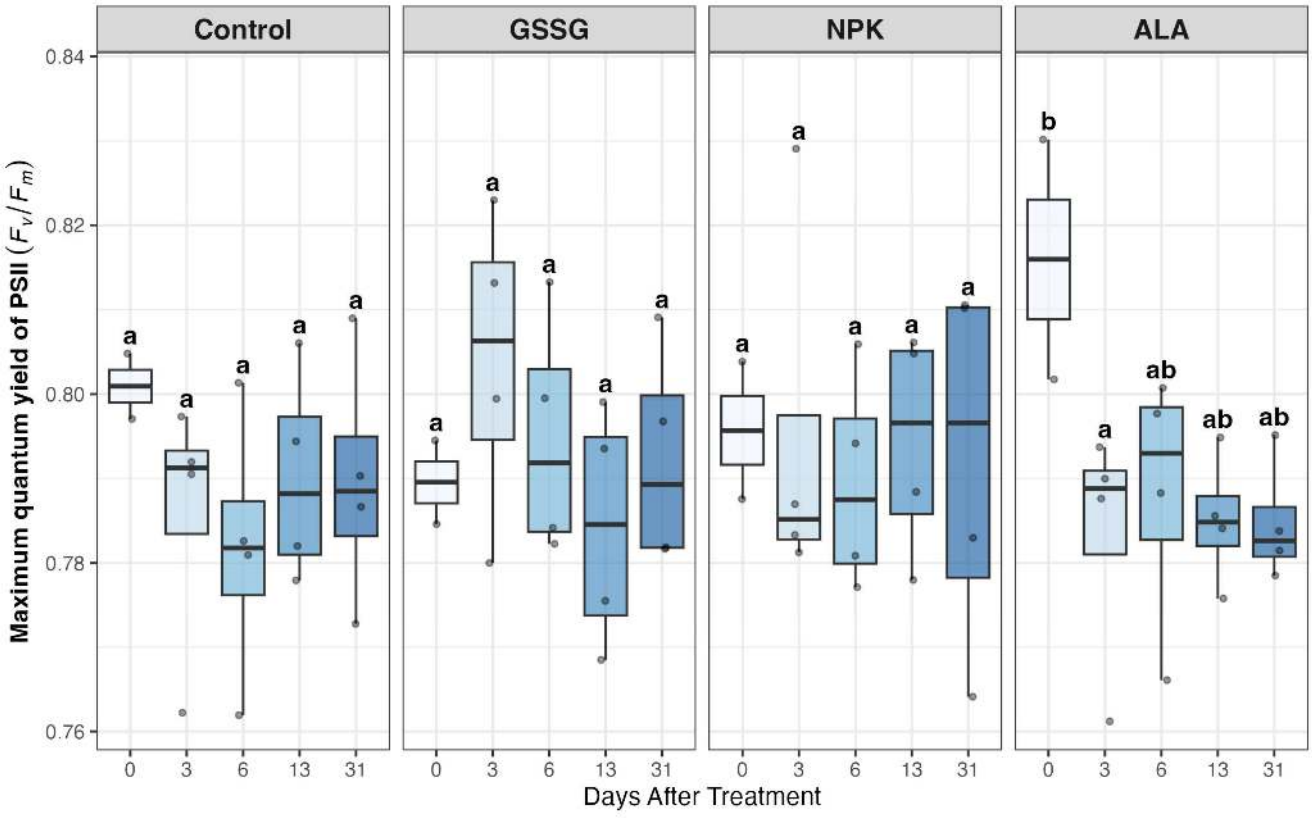

(b)

Figure 2. *Cont.*

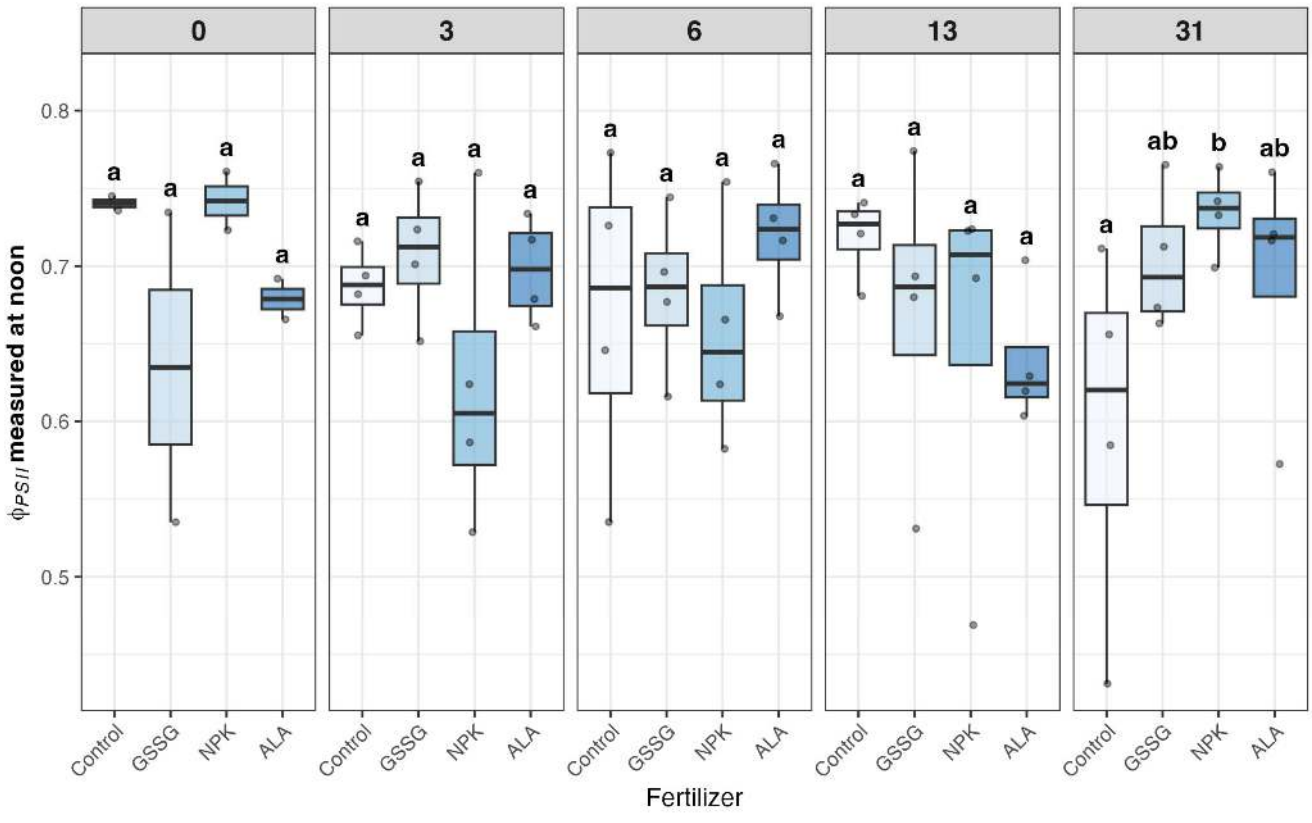

(c)

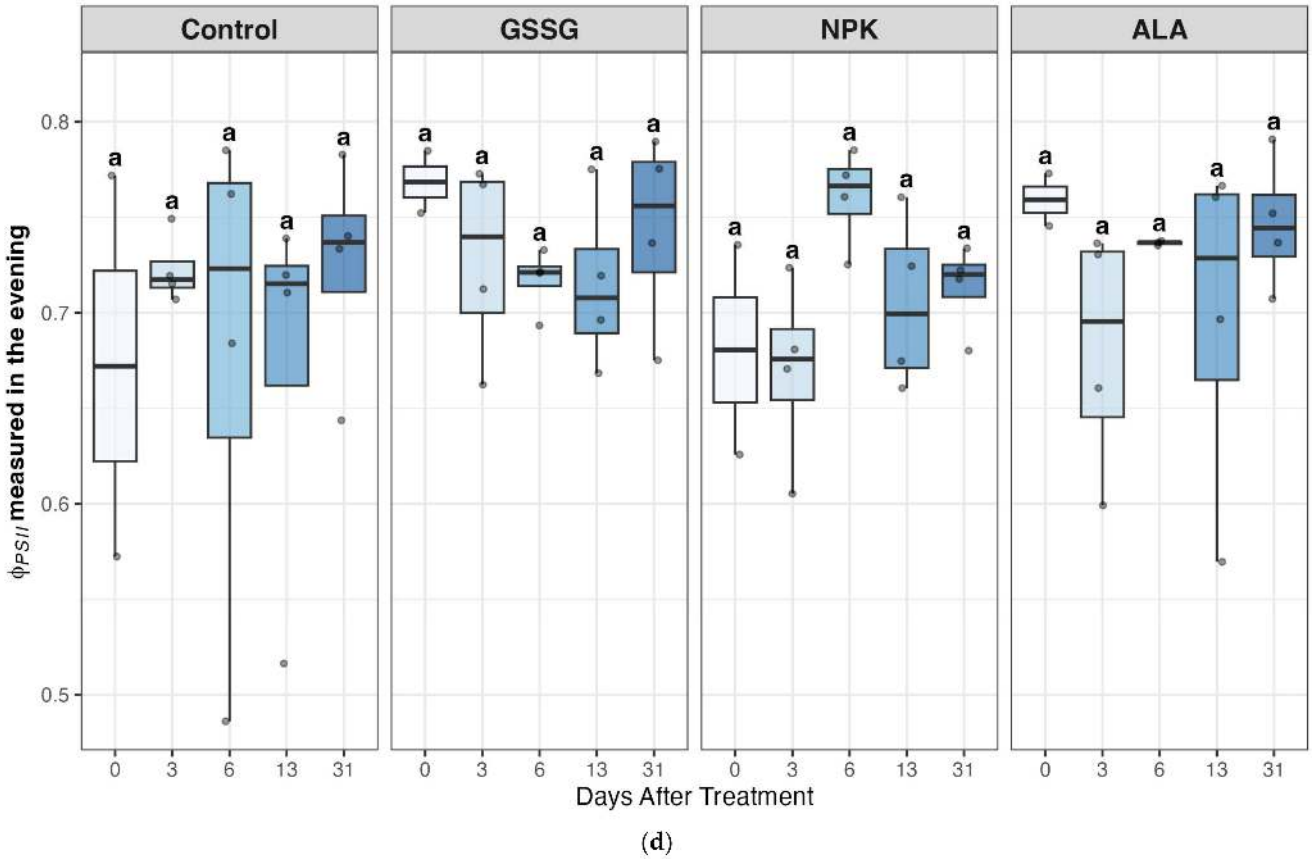

(d)

Figure 2. *Cont.*

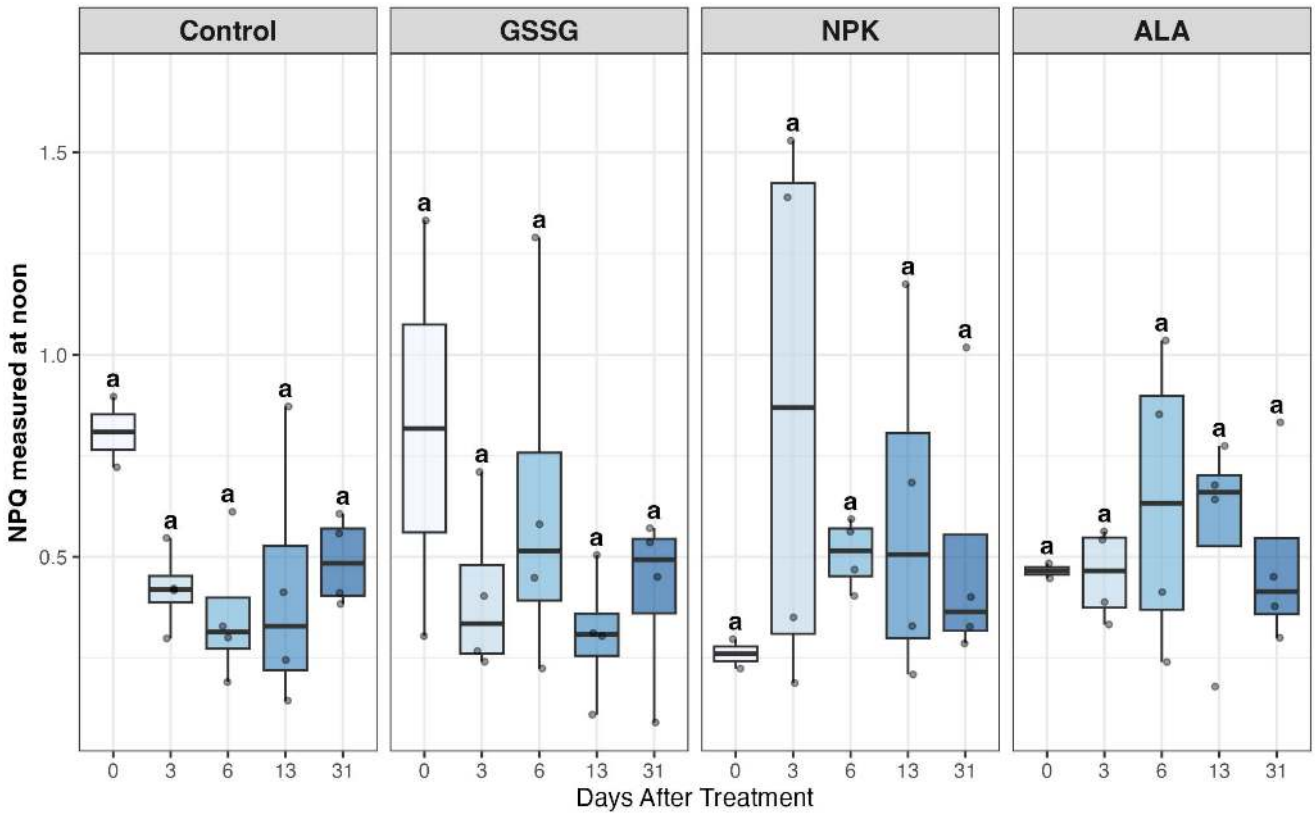

(e)

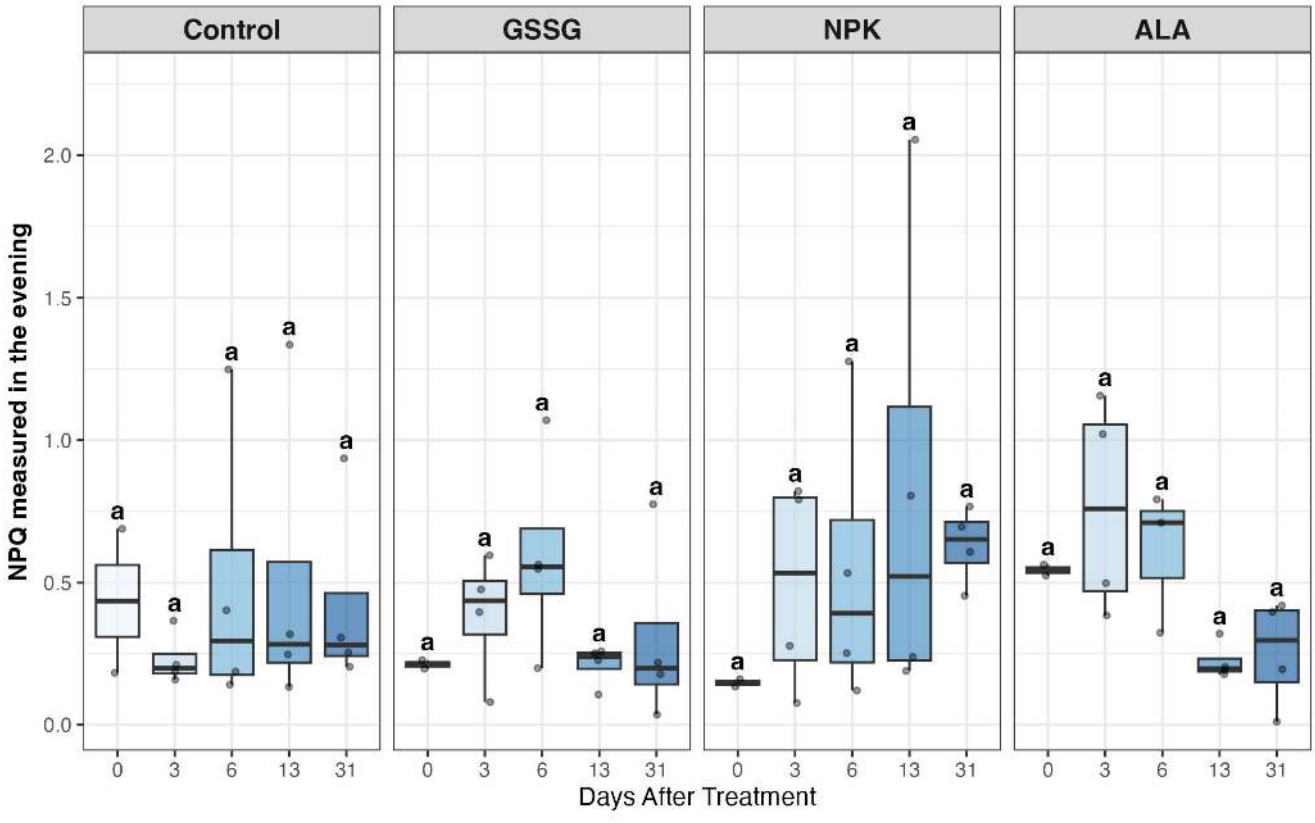

(f)

Figure 2. Graphical representation of the linear mixed-effects models for leaf gas exchange and chlorophyll fluorescence traits. Pairwise contrasts between fertilizer treatment and observation time were performed separately for each fertilizer. Shown are the maximum photosynthetic rate at light

saturation (A_{max}) (**a**), maximum quantum yield of PSII (F_v/F_m) (**b**), quantum yield of PSII (Φ_{PSII}) measured at noon (12:00) (**c**) and in the evening (17:00) (**d**), and non-photochemical quenching (NPQ) measured at noon (12:00) (**e**) and in the evening (17:00) (**f**). Different letters indicate significant differences among groups based on estimated marginal means, with *p*-values adjusted for multiple comparisons using Tukey's method ($p < 0.05$). Points represent the distribution of individual data points.

Table 3. Pairwise comparisons of the maximum quantum yield of PSII (F_v/F_m) between observation times within each fertilizer treatment, using Tukey's adjustment for multiple comparisons.

Contrast	Estimate (β)	Std. Error	df	*t* Ratio	*p* Value
Fertilizer: Control					
Day0–Day3	0.022	0.009	41.08141889	2.42	0.1298
Day0–Day6	0.026	0.009	41.08141889	2.84	0.0517
Day0–Day13	0.018	0.009	41.08141889	1.92	0.3232
Day0–Day31	0.018	0.009	41.08141889	1.97	0.3001
Day3–Day6	0.004	0.007	40.00344317	0.53	0.9839
Day3–Day13	−0.005	0.007	40.00344317	−0.64	0.9679
Day3–Day31	−0.004	0.007	40.00344317	−0.58	0.9775
Day6–Day13	−0.008	0.007	40.00344317	−1.17	0.7702
Day6–Day31	−0.008	0.007	40.00344317	−1.11	0.8018
Day13–Day31	0	0.007	40.00344317	0.06	1
Fertilizer: GSSG					
Day0–Day3	−0.014	0.009	41.08141889	−1.57	0.5236
Day0–Day6	−0.005	0.009	41.08141889	−0.58	0.9779
Day0–Day13	0.005	0.009	41.08141889	0.59	0.976
Day0–Day31	**−0.003**	0.009	41.08141889	−0.31	**0.998**
Day3–Day6	0.009	0.007	40.00344317	1.26	0.714
Day3–Day13	**0.02**	0.007	40.00344317	**2.74**	**0.065**
Day3–Day31	0.012	0.007	40.00344317	1.61	0.5028
Day6–Day13	0.011	0.007	40.00344317	1.48	0.5817
Day6–Day31	0.002	0.007	40.00344317	0.34	0.997
Day13–Day31	−0.008	0.007	40.00344317	−1.14	0.7855
Fertilizer: NPK					
Day0–Day3	−0.001	0.009	41.08141889	−0.14	0.9999
Day0–Day6	0.004	0.009	41.08141889	0.47	0.9893
Day0–Day13	0	0.009	41.08141889	−0.05	1
Day0–Day31	0.002	0.009	41.08141889	0.21	0.9996
Day3–Day6	0.006	0.007	40.00344317	0.78	0.9342
Day3–Day13	0.001	0.007	40.00344317	0.11	1
Day3–Day31	0.003	0.007	40.00344317	0.44	0.9916
Day6–Day13	−0.005	0.007	40.00344317	−0.67	0.9622
Day6–Day31	−0.002	0.007	40.00344317	−0.34	0.9971
Day13–Day31	0.002	0.007	40.00344317	0.33	0.9973
Fertilizer: ALA					
Day0–Day3	0.027	0.009	41.08141889	2.92	0.0422
Day0–Day6	0.022	0.009	41.08141889	2.37	0.1444
Day0–Day13	0.025	0.009	41.08141889	2.71	0.0697
Day0–Day31	0.025	0.009	41.08141889	2.75	0.0637
Day3–Day6	−0.005	0.007	40.00344317	−0.7	0.9544
Day3–Day13	−0.002	0.007	40.00344317	−0.27	0.9987
Day3–Day31	−0.002	0.007	40.00344317	−0.22	0.9994
Day6–Day13	0.003	0.007	40.00344317	0.43	0.9925
Day6–Day31	0.003	0.007	40.00344317	0.48	0.9886
Day13–Day31	0	0.007	40.00344317	0.05	1

Table 4. Linear mixed-effects model results for the effects of fertilizer treatment and observation time (Day) on the maximum quantum yield of PSII (F_v/F_m). F_v/F_m was modeled with Fertilizer and Day as fixed factors and Plant_No as a random effect. *p*-values were calculated using Satterthwaite's method. The intercept represents the baseline group (Control Fertilizer at Day 0). Asterisks indicate significance: *** $p < 0.001$, ** $p < 0.01$, * $p < 0.05$, . $p < 0.1$.

Term	Estimate (β)	Std. Error	df	*t* Value	*p* Value	Sig
Fixed effects						
(Intercept)	0.807649	0.009358	42.738497	86.308	<0.001	***
Fertilizer Main Effects						
Fertilizer (GSSG)	−0.018108	0.013234	42.738497	−1.368	0.17836	
Fertilizer (NPK)	−0.013794	0.013234	42.738497	−1.042	0.30311	
Fertilizer (ALA)	0.002207	0.013234	42.738497	0.167	0.86832	
Day Main Effects						
Day 3	−0.022137	0.009113	41.274762	−2.429	0.01957	*
Day 6	−0.025942	0.009113	41.274762	−2.847	0.00685	**
Day 13	−0.017548	0.009113	41.274762	−1.926	0.06106	.
Day 31	−0.017973	0.009113	41.274762	−1.972	0.0553	.
Interactions: Fertilizer × Day 3						
GSSG × Day 3	0.036499	0.012888	41.274762	2.832	**0.00712**	**
NPK × Day 3	0.023439	0.012888	41.274762	1.819	0.07622	.
ALA × Day 3	−0.004584	0.012888	41.274762	−0.356	0.72388	
Interactions: Fertilizer × Day 6						
GSSG × Day 6	0.031204	0.012888	41.274762	2.421	**0.01995**	*
NPK × Day 6	0.021612	0.012888	41.274762	1.677	0.1011	
ALA × Day 6	0.004286	0.012888	41.274762	0.333	0.74115	
Interactions: Fertilizer × Day 13						
GSSG × Day 13	0.012164	0.012888	41.274762	0.944	0.35074	
NPK × Day 13	0.018022	0.012888	41.274762	1.398	0.16947	
ALA × Day 13	−0.007217	0.012888	41.274762	−0.56	0.57853	
Interactions: Fertilizer × Day 31						
GSSG × Day 31	0.020781	0.012888	41.274762	1.612	0.11448	
NPK × Day 31	0.016074	0.012888	41.274762	1.247	0.21933	
ALA × Day 31	−0.00715	0.012888	41.274762	−0.555	0.58205	
Random effects						
Groups Name	**Variance**	**Std. Dev.**				
Plant_No (Intercept)	0.0001217	0.01103				
Residual	0.0001036	0.01018				

On Day 31, the linear mixed-effects model showed a significant interaction between the GSSG treatment and day ($p = 0.019$) for Φ_{PSII} measured at noon (Table 6). The positive estimate (0.211) suggests that the GSSG group maintained significantly higher efficiency on that specific day (Table 6). However, following Tukey's adjustment for multiple comparisons, noon Φ_{PSII} in the GSSG treatment did not differ statistically from the other fertilizers or the control during the first two weeks (Figure 2c, Table S10). By the end of the observation period, the GSSG treatment showed higher noon Φ_{PSII} than the control, although this difference was not statistically significant relative to other fertilizer treatments (Figure 2c, Table S10).

Table 5. Pairwise comparisons of the maximum quantum yield of PSII (F_v/F_m) between fertilizer treatments within each observation time, using Tukey's adjustment for multiple comparisons.

Contrast	Estimate (β)	Std. Error	df	t Ratio	p Value
Day 0					
Control–GSSG	0.018	0.013	42.56550969	1.36	0.528
Control–NPK	0.014	0.013	42.56550969	1.04	0.7274
Control–ALA	−0.002	0.013	42.56550969	−0.17	0.9983
GSSG–NPK	−0.004	0.013	42.56550969	−0.33	0.988
GSSG–ALA	−0.02	0.013	42.56550969	−1.53	0.4285
NPK–ALA	−0.016	0.013	42.56550969	−1.21	0.6266
Day 3					
Control–GSSG	−0.018	0.011	26.30474086	−1.73	0.3276
Control–NPK	−0.01	0.011	26.30474086	−0.91	0.8004
Control–ALA	0.002	0.011	26.30474086	0.22	0.9959
GSSG–NPK	0.009	0.011	26.30474086	0.82	0.8426
GSSG–ALA	0.021	0.011	26.30474086	1.96	0.2298
NPK–ALA	0.012	0.011	26.30474086	1.13	0.6731
Day 6					
Control–GSSG	−0.013	0.011	26.30474086	−1.23	0.6116
Control–NPK	−0.008	0.011	26.30474086	−0.74	0.8815
Control–ALA	−0.006	0.011	26.30474086	−0.61	0.9274
GSSG–NPK	0.005	0.011	26.30474086	0.5	0.959
GSSG–ALA	0.007	0.011	26.30474086	0.62	0.9241
NPK–ALA	0.001	0.011	26.30474086	0.12	0.9993
Day 13					
Control–GSSG	0.006	0.011	26.30474086	0.56	0.9429
Control–NPK	−0.004	0.011	26.30474086	−0.4	0.9782
Control–ALA	0.005	0.011	26.30474086	0.47	0.9646
GSSG–NPK	−0.01	0.011	26.30474086	−0.96	0.7738
GSSG–ALA	−0.001	0.011	26.30474086	−0.09	0.9997
NPK–ALA	0.009	0.011	26.30474086	0.87	0.8201
Day 31					
Control–GSSG	−0.003	0.011	26.30474086	−0.25	0.9943
Control–NPK	−0.002	0.011	26.30474086	−0.21	0.9964
Control–ALA	0.005	0.011	26.30474086	0.47	0.9659
GSSG–NPK	0	0.011	26.30474086	0.04	1
GSSG–ALA	0.008	0.011	26.30474086	0.72	0.8893
NPK–ALA	0.007	0.011	26.30474086	0.68	0.9036

3.3. Nitrogen-Related Traits

In this study, GSSG application exerted varying effects on nitrogen (N) content, carbon (C) content, and carbon-to-nitrogen (C:N) ratio over a 31-day period (Figure 3a–c). However, no significant effect on PNUE was observed (Figure 3d). Post hoc pairwise comparisons (Tukey-adjusted) revealed no significant differences in nitrogen percentage among fertilizer treatments at any observation time point (Table S14), consistent with the lack of a significant interaction between Fertilizer and Day in the linear mixed-effects model (Table 7). Although inter-treatment differences were not significant on any given day, the temporal dynamics of nitrogen accumulation varied with the treatments (Figure 3a, Table S25). Saplings treated with GSSG exhibited a gradual increase in nitrogen content, reaching a significant peak on Day 13 relative to baseline levels (Figure 3a). Regarding carbon concentration, GSSG treatment induced a significant temporal shift (Figure 3b), with levels peaking on Day 3 before undergoing a significant decline by Days 6 and 31 (Figure 3b, Table S26). Despite these internal fluctuations, the carbon percentage in the GSSG-treated saplings did not differ significantly from that of the control or other fertilizer groups at any stage of the experiment (Table S15).

Table 6. Linear mixed-effects model results for the effects of fertilizer treatment and observation time (Day) on the quantum yield of PSII (Φ_{PSII}) measured at noon (12:00). Noon Φ_{PSII} was modeled with Fertilizer and Day as fixed factors and Plant_No as a random effect. *p*-values were calculated using Satterthwaite's method. The intercept represents the baseline group (Control Fertilizer at Day 0). Asterisks indicate significance: *** $p < 0.001$, * $p < 0.05$, . $p < 0.1$.

Term	Estimate (β)	Std. Error	df	*t* Value	*p* Value	Sig
Fixed effects						
(Intercept)	0.73331	0.0516	51.99997	14.21	<0.001	***
Fertilizer Main Effects						
Fertilizer (GSSG)	−0.1038	0.07298	51.99997	−1.422	0.1609	
Fertilizer (NPK)	0.01976	0.07298	51.99997	0.271	0.7877	
Fertilizer (ALA)	−0.05592	0.07298	51.99997	−0.766	0.447	
Day Main Effects						
Day 3	−0.04648	0.0614	43.71885	−0.757	0.4531	
Day 6	−0.0633	0.0614	43.71885	−1.031	0.3082	
Day 13	−0.01439	0.0614	43.71885	−0.234	0.8158	
Day 31	**−0.13755**	0.0614	43.71885	−2.24	0.0302	*
Interactions: Fertilizer × Day 3						
GSSG × Day 3	0.12464	0.08683	43.71885	1.435	0.1583	
NPK × Day 3	−0.08179	0.08683	43.71885	−0.942	0.3514	
ALA × Day 3	0.06677	0.08683	43.71885	0.769	0.446	
Interactions: Fertilizer × Day 6						
GSSG × Day 6	0.11718	0.08683	43.71885	1.35	0.1841	
NPK × Day 6	−0.03325	0.08683	43.71885	−0.383	0.7036	
ALA × Day 6	0.10617	0.08683	43.71885	1.223	0.228	
Interactions: Fertilizer × Day 13						
GSSG × Day 13	0.05447	0.08683	43.71885	0.627	0.5337	
NPK × Day 13	−0.08677	0.08683	43.71885	−0.999	0.3232	
ALA × Day 13	−0.02397	0.08683	43.71885	−0.276	0.7838	
Interactions: Fertilizer × Day 31						
GSSG × Day 31	**0.21159**	0.08683	43.71885	2.437	**0.019**	*
NPK × Day 31	0.11881	0.08683	43.71885	1.368	0.1782	
ALA × Day 31	0.15263	0.08683	43.71885	1.758	0.0858	.
Random effects						
Groups Name	**Variance**	**Std. Dev.**				
Plant_No (Intercept)	0.000484	0.022				
Residual	0.004911	0.07008				

The C:N ratio showed no significant differences among fertilizer treatments at any observation time point (Table S16), which is consistent with the lack of a significant interaction between Fertilizer and Day in the linear mixed-effects model, except on Day 6 (Table S4). However, internal temporal patterns varied significantly over time (Figure 3c). Post hoc comparisons indicated that while the control group showed a significant reduction in the C:N ratio by Day 6, the GSSG treatment did not show a significant decrease from baseline until Day 13 (Figure 3c, Table S27). Consistent with these nitrogen-related traits, GSSG treatment did not significantly alter PNUE compared with the control at any observation time point (Table S17).

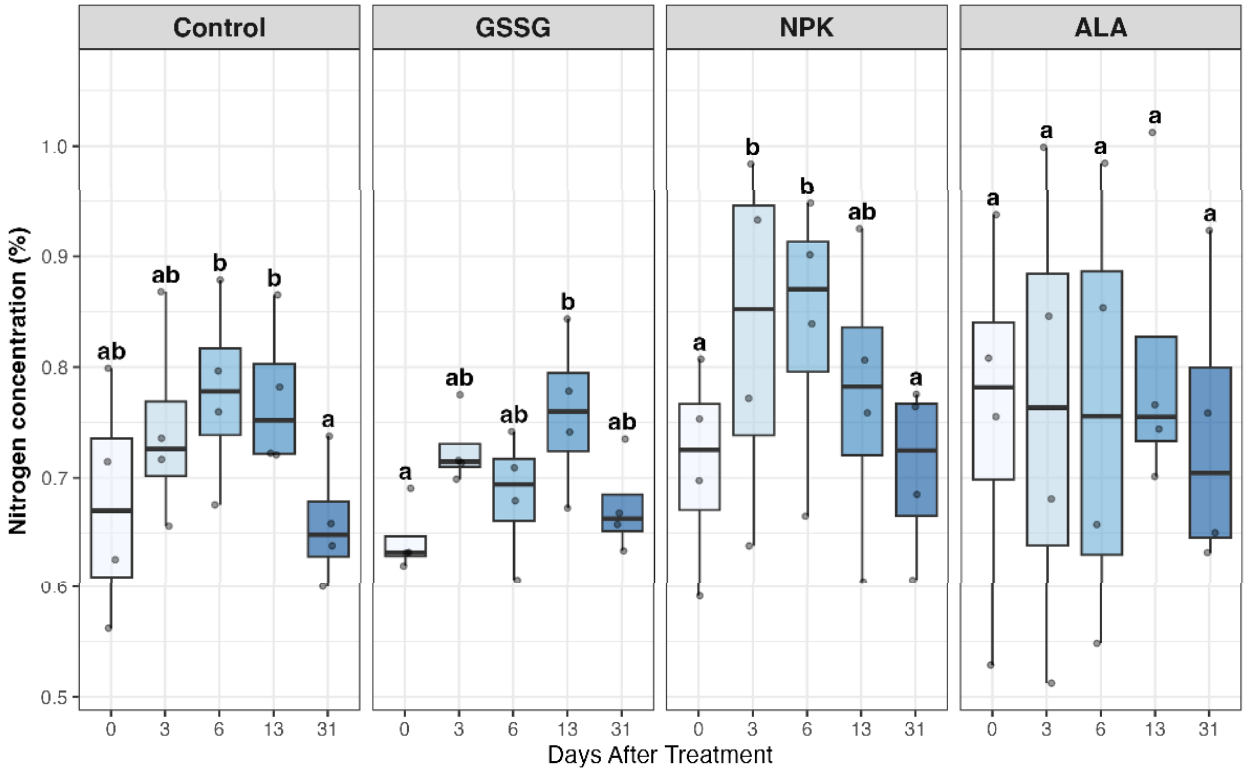

(**a**)

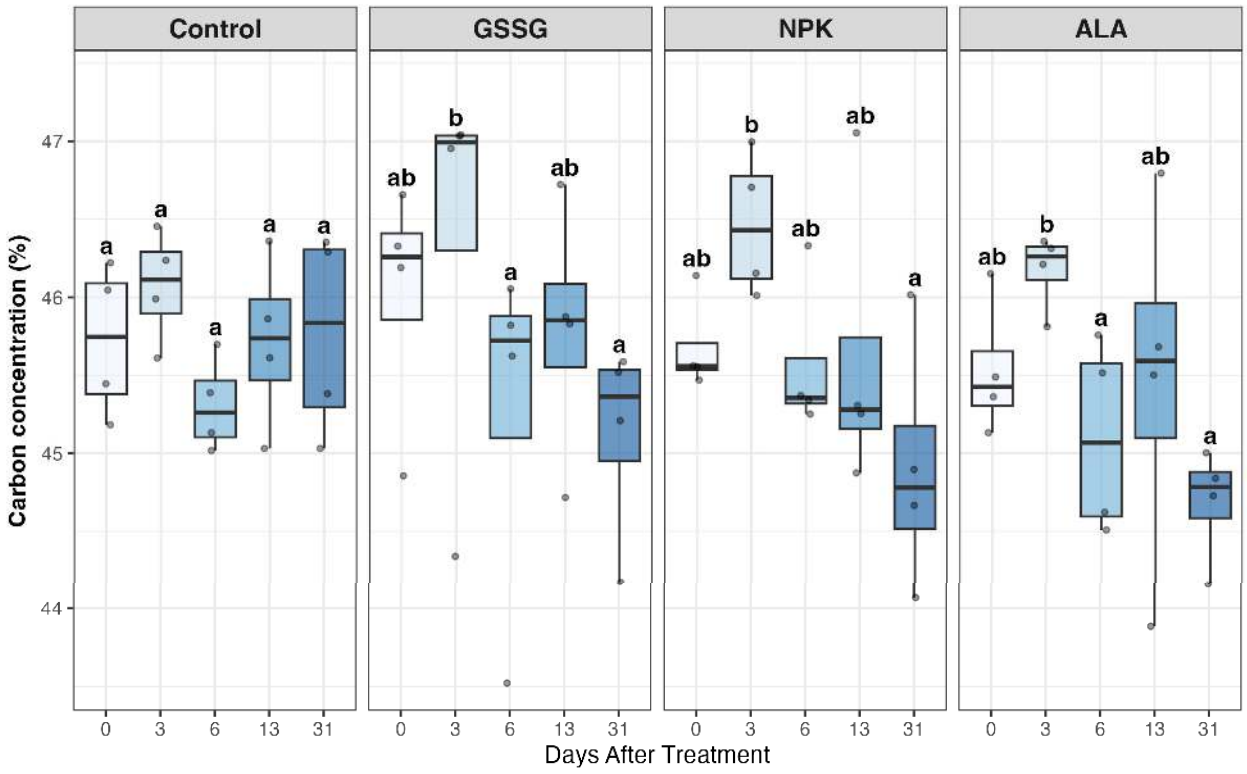

(**b**)

Figure 3. *Cont.*

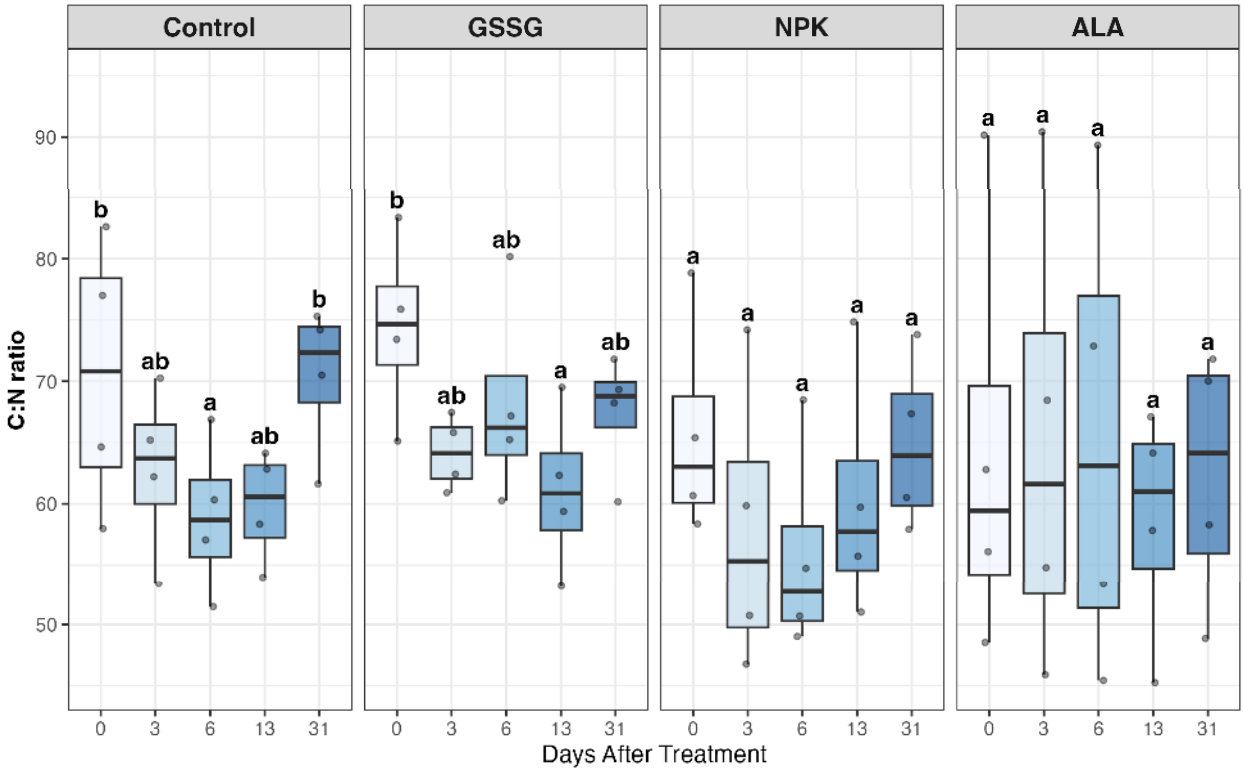

(**c**)

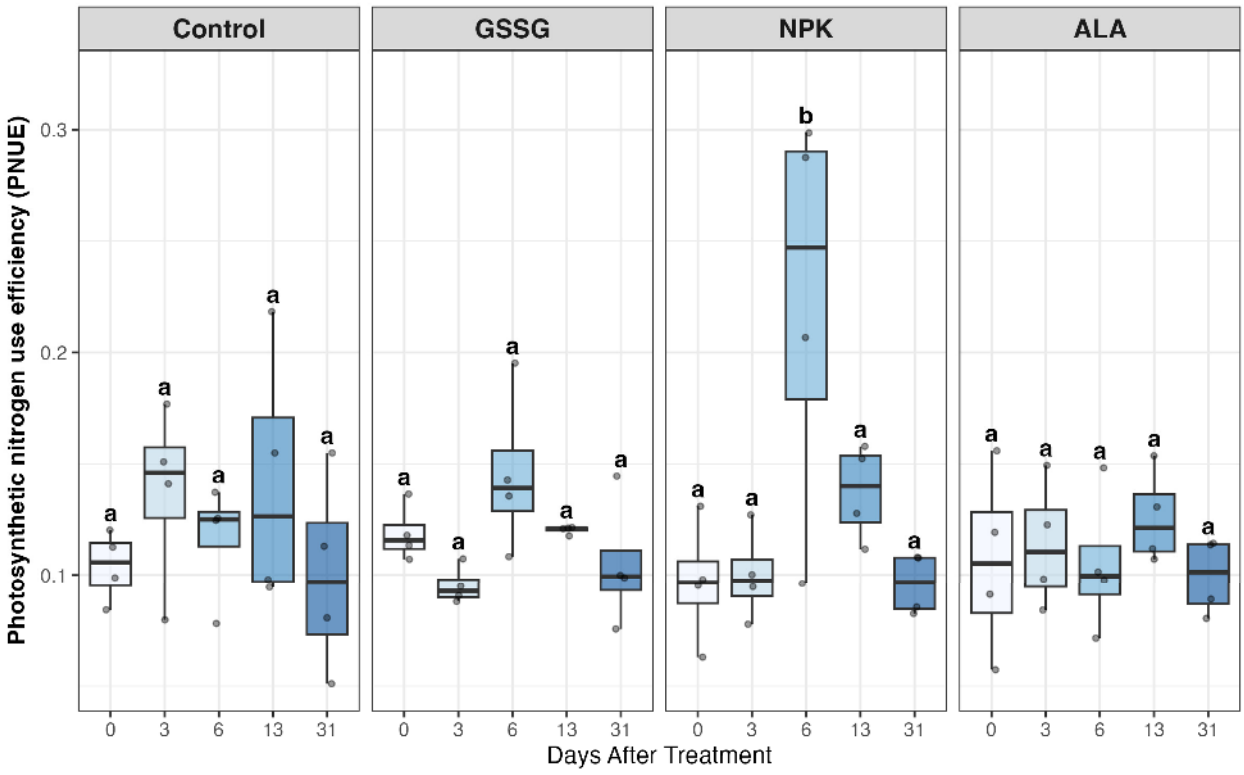

(**d**)

Figure 3. Graphical representation of the linear mixed-effects models for nitrogen-related traits. Pairwise contrasts between fertilizer treatment and observation time were performed separately for each fertilizer. Shown are nitrogen concentration (**a**), carbon concentration (**b**), C:N ratio (**c**), and photosynthetic nitrogen use efficiency (PNUE) (**d**). Different letters indicate significant differences among groups based on estimated marginal means, with *p*-values adjusted for multiple comparisons using Tukey's method ($p < 0.05$). Points represent the distribution of individual data points.

Table 7. Linear mixed-effects model results for the effects of fertilizer treatment and observation time (Day) on nitrogen concentration. Nitrogen concentration was modeled with Fertilizer and Day as fixed factors and Plant_No as a random effect. *p*-values were calculated using Satterthwaite's method. The intercept represents the baseline group (Control Fertilizer at Day 0). Asterisks indicate significance: *** $p < 0.001$, ** $p < 0.01$, * $p < 0.05$, . $p < 0.1$.

Term	Estimate (β)	Std. Error	df	*t* Value	*p* Value	Sig
Fixed effects						
(Intercept)	0.6753804	0.0577689	17.2418008	11.691	<0.001	***
Fertilizer Main Effects						
Fertilizer (GSSG)	−0.0314779	0.0816976	17.2418008	−0.385	0.70473	
Fertilizer (NPK)	0.0369462	0.0816976	17.2418008	0.452	0.65674	
Fertilizer (ALA)	0.0820217	0.0816976	17.2418008	1.004	0.32928	
Day Main Effects						
Day 3	0.0688017	0.0376707	48	1.826	0.07401	.
Day 6	0.10219	0.0376707	48	2.713	0.00924	**
Day 13	0.0971289	0.0376707	48	2.578	0.01305	*
Day 31	−0.016609	0.0376707	48	−0.441	0.66126	
Interactions: Fertilizer × Day 3						
GSSG × Day 3	0.0130272	0.0532744	48	0.245	0.80786	
NPK × Day 3	0.0506355	0.0532744	48	0.95	0.34664	
ALA × Day 3	−0.0666476	0.0532744	48	−1.251	0.21699	
Interactions: Fertilizer × Day 6						
GSSG × Day 6	−0.0617343	0.0532744	48	−1.159	0.25227	
NPK × Day 6	0.0239544	0.0532744	48	0.45	0.65499	
ALA × Day 6	−0.0985109	0.0532744	48	−1.849	0.0706	.
Interactions: Fertilizer × Day 13						
GSSG × Day 13	0.0178928	0.0532744	48	0.336	0.73844	
NPK × Day 13	−0.0355593	0.0532744	48	−0.667	0.50767	
ALA × Day 13	−0.0486797	0.0532744	48	−0.914	0.36541	
Interactions: Fertilizer × Day 31						
GSSG × Day 31	0.0464744	0.0532744	48	0.872	0.38736	
NPK × Day 31	0.0122606	0.0532744	48	0.23	0.81896	
ALA × Day 31	0.0003783	0.0532744	48	0.007	0.99436	
Random effects						
Groups Name	**Variance**	**Std. Dev.**				
Plant_No (Intercept)	0.010511	0.10252				
Residual	0.002838	0.05327				

3.4. Growth and Biomass

Despite any significance observed in the linear mixed-effects model (Tables S6 and S7), post hoc analysis showed that GSSG application had no significant effect on sapling height or stem diameter throughout the 31-day study period (Figure 4a,b, Tables S29 and S30). Consistent with these results, no significant differences were observed in the 2024 terminal shoot or the 2024 annual ring width (Figure 4c,d), following Tukey's adjustment (Tables S18 and S19). Regarding biomass allocation, the GSSG-treated group exhibited higher stem biomass than the other groups (Table 8), although these differences were not statistically significant (Figure 5a, Table 8).

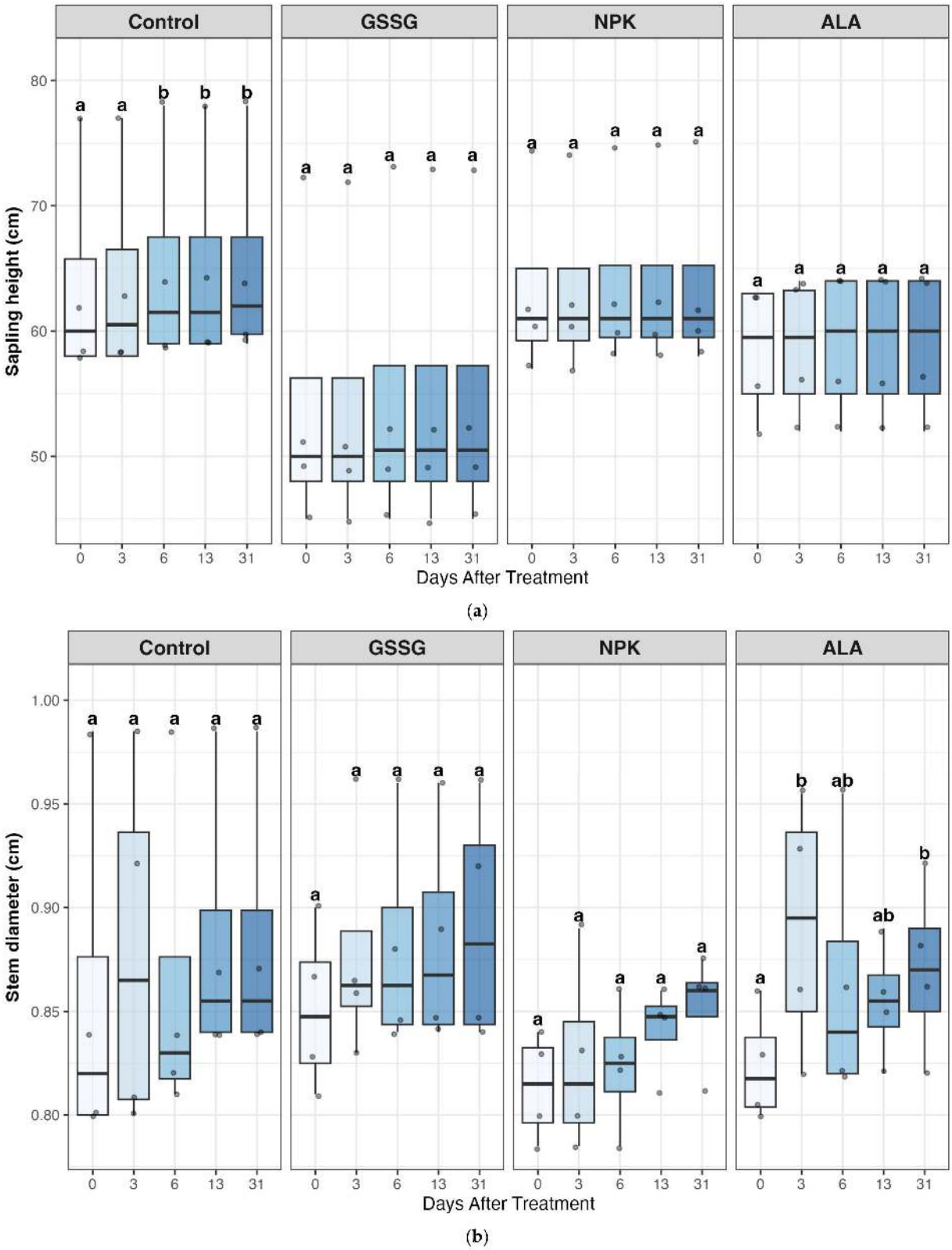

Figure 4. *Cont.*

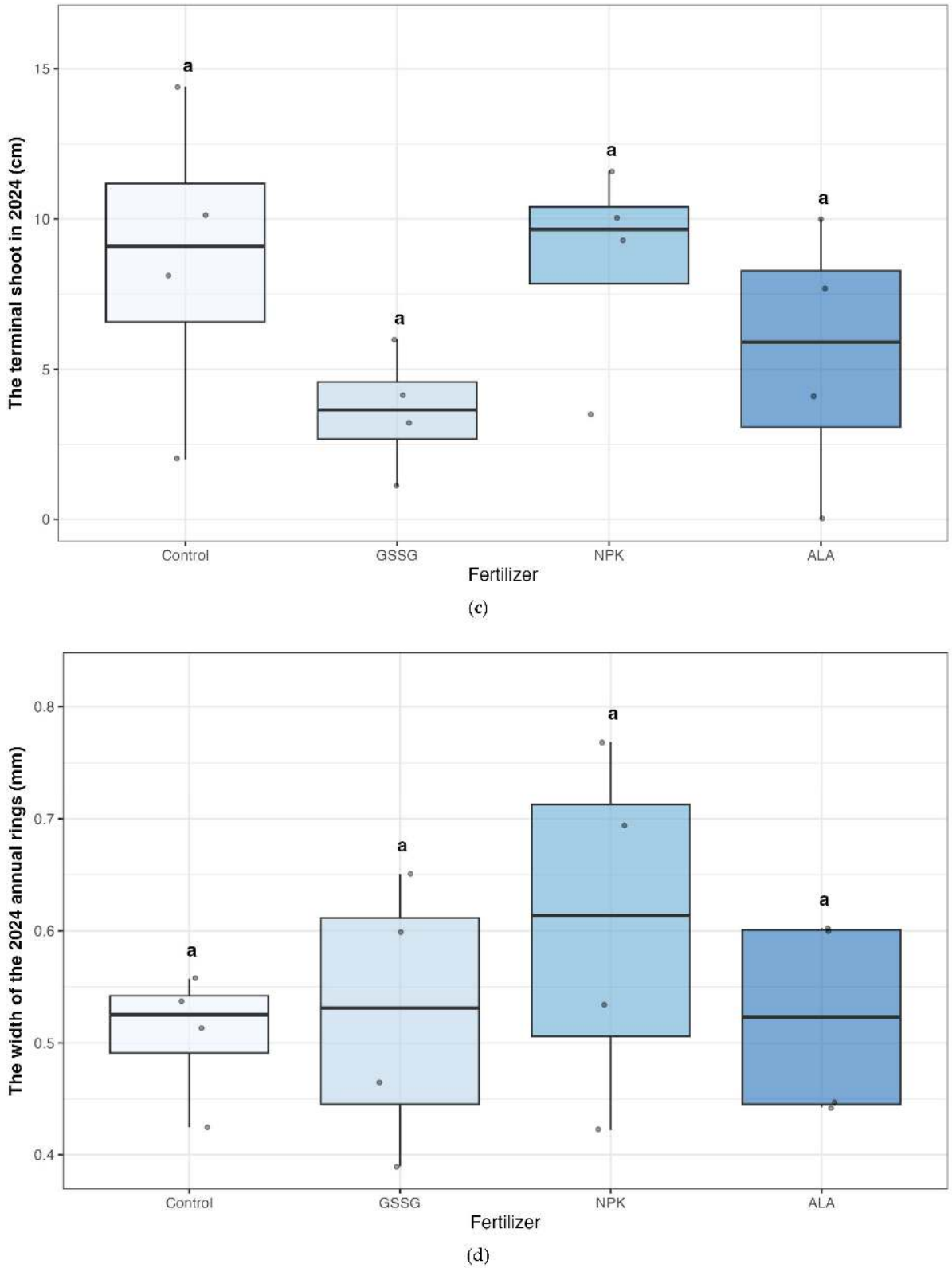

Figure 4. Graphical representation of the linear mixed-effects models for growth traits. Pairwise contrasts between fertilizer treatment and observation time were performed separately for each fertilizer for sapling height (**a**) and stem diameter (**b**). Comparisons among fertilizer treatments were performed for the terminal shoot in 2024 (**c**) and the width of the 2024 annual ring (**d**). Different letters indicate significant differences among groups based on estimated marginal means, with *p*-values adjusted for multiple comparisons using Tukey's method ($p < 0.05$). Points represent the distribution of individual data points.

Table 8. Pairwise comparisons of 2024 growth increment (annual ring width and shoot length), and biomass between fertilizer treatments three months after treatment, using Tukey's adjustment for multiple comparisons.

Contrast	Estimate (β)	Std. Error	df	t Ratio	p Value
The width of 2024 annual ring					
Control–GSSG	−0.0176	0.0794	12	−0.2219	0.9959
Control–NPK	−0.0967	0.0794	12	−1.2172	0.6283
Control–ALA	−0.0149	0.0794	12	−0.1881	0.9975
GSSG–NPK	−0.0791	0.0794	12	−0.9953	0.7549
GSSG–ALA	0.0027	0.0794	12	0.0338	1.0000
NPK–ALA	0.0818	0.0794	12	1.0292	0.7362
The terminal shoot in 2024					
Control–GSSG	5.05	2.7903	12	1.8098	0.3156
Control–NPK	0.05	2.7903	12	0.0179	1.0000
Control–ALA	3.2	2.7903	12	1.1468	0.6693
GSSG–NPK	−5	2.7903	12	−1.7919	0.3234
GSSG–ALA	−1.85	2.7903	12	−0.6630	0.9089
NPK–ALA	3.15	2.7903	12	1.1289	0.6796
The biomass of stem within the terminal shoot in 2024					
Control–GSSG	**−0.1418**	0.1025	12	−1.3834	0.5321
Control–NPK	0.026	0.1025	12	0.2537	0.9940
Control–ALA	0.0667	0.1025	12	0.6514	0.9130
GSSG–NPK	**0.1678**	0.1025	12	1.6371	0.3958
GSSG–ALA	**0.2085**	0.1025	12	2.0348	0.2291
NPK–ALA	0.0408	0.1025	12	0.3977	0.9777
The biomass of needles within the terminal shoot in 2024					
Control–GSSG	0.0315	0.0649	12	0.4856	0.9608
Control–NPK	0.002	0.0649	12	0.0308	1.0000
Control–ALA	0.049	0.0649	12	0.7554	0.8727
GSSG–NPK	−0.0295	0.0649	12	−0.4548	0.9674
GSSG–ALA	0.0175	0.0649	12	0.2698	0.9928
NPK–ALA	0.047	0.0649	12	0.7245	0.8854
Total stem biomass					
Control–GSSG	0.376	0.6522	12	0.5765	0.9372
Control–NPK	−0.058	0.6522	12	−0.0889	0.9997
Control–ALA	0.8655	0.6522	12	1.3271	0.5644
GSSG–NPK	−0.434	0.6522	12	−0.6654	0.9080
GSSG–ALA	0.4895	0.6522	12	0.7505	0.8747
NPK–ALA	0.9235	0.6522	12	1.4160	0.5136
Total needles biomass					
Control–GSSG	0.6395	0.6839	12	0.9351	0.7870
Control–NPK	0.2	0.6839	12	0.2925	0.9908
Control–ALA	0.4725	0.6839	12	0.6909	0.8986
GSSG–NPK	−0.4395	0.6839	12	−0.6427	0.9161
GSSG–ALA	−0.167	0.6839	12	−0.2442	0.9946
NPK–ALA	0.2725	0.6839	12	0.3985	0.9776
Root biomass					
Control–GSSG	**−1.6308**	0.9786	12	−1.6665	0.3814
Control–NPK	−0.7848	0.9786	12	−0.8019	0.8522
Control–ALA	−0.2395	0.9786	12	−0.2447	0.9946
GSSG–NPK	**0.846**	0.9786	12	0.8645	0.8227
GSSG–ALA	**1.3913**	0.9786	12	1.4217	0.5104
NPK–ALA	0.5453	0.9786	12	0.5572	0.9428

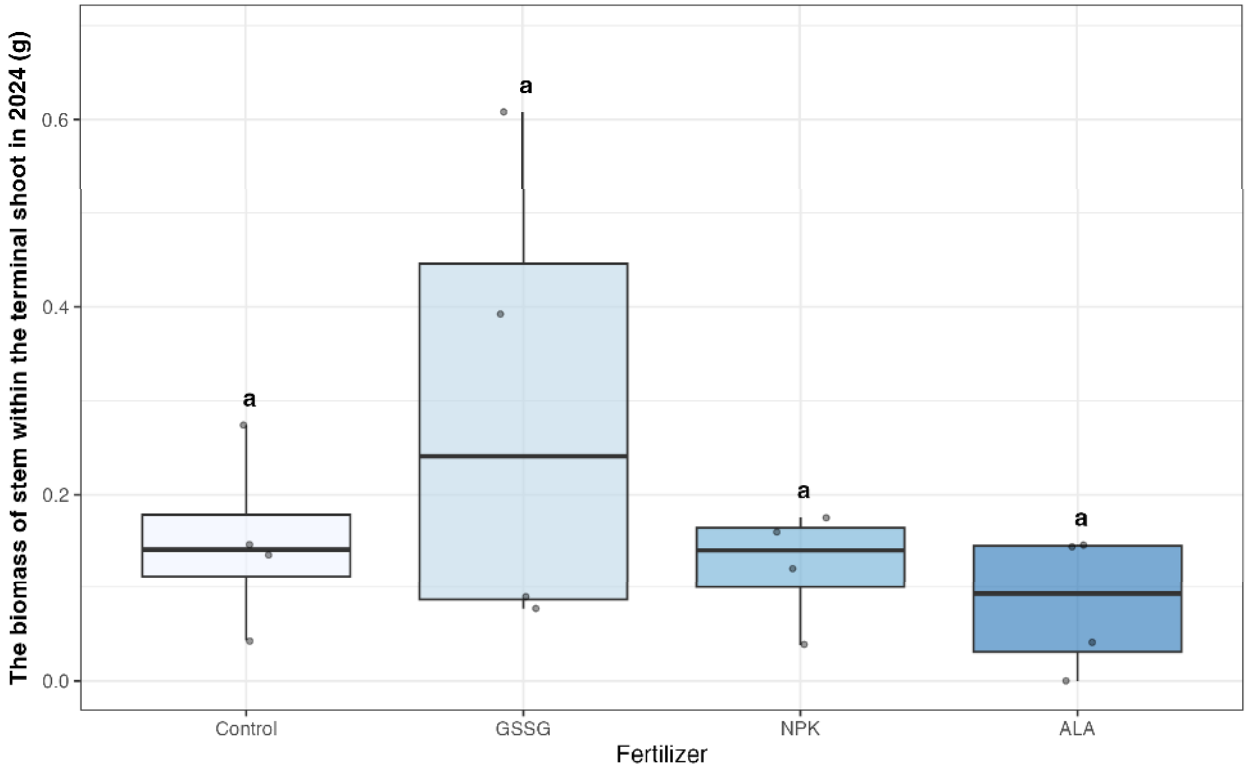

(**a**)

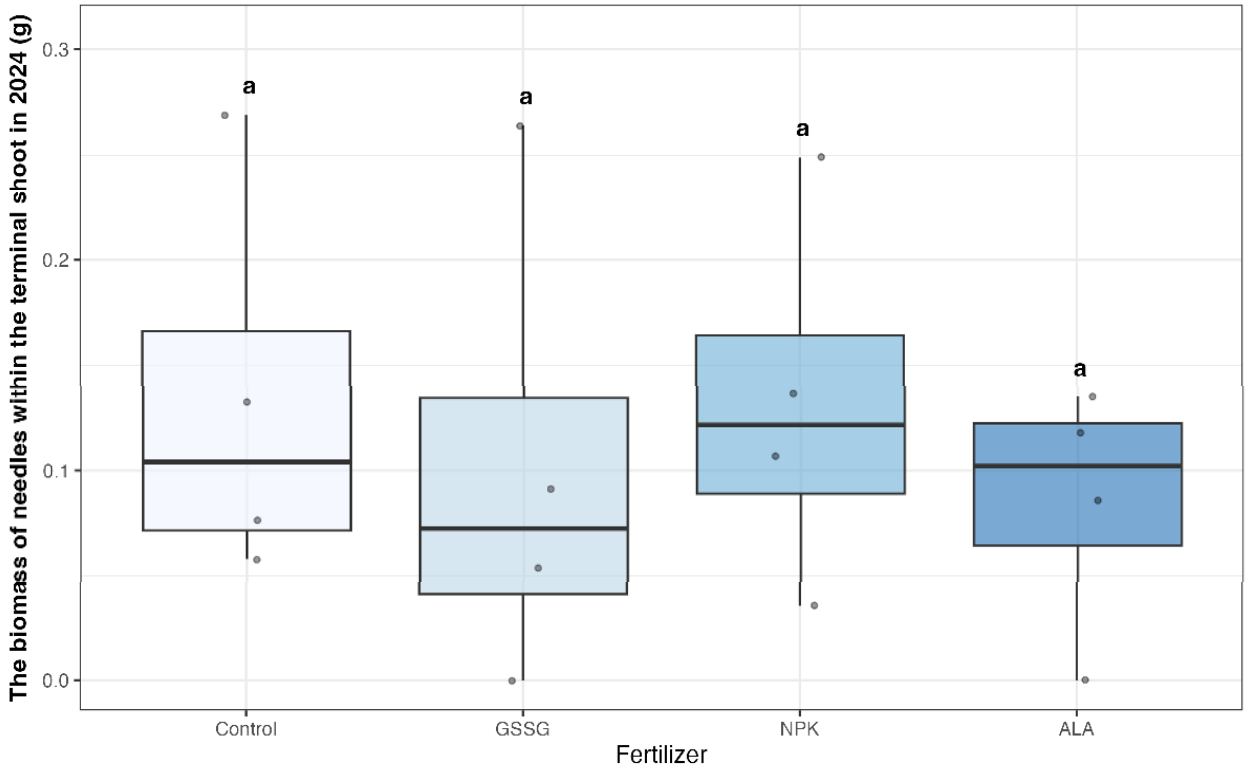

(**b**)

Figure 5. *Cont.*

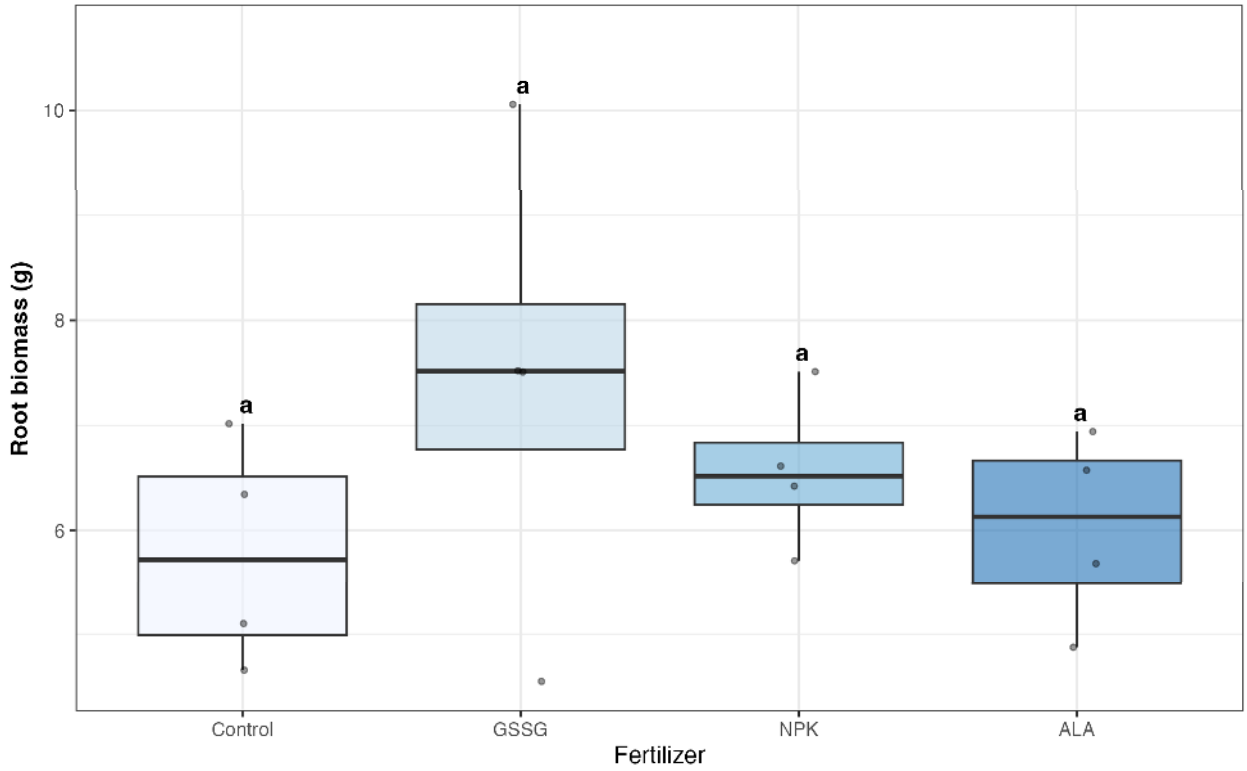

(**c**)

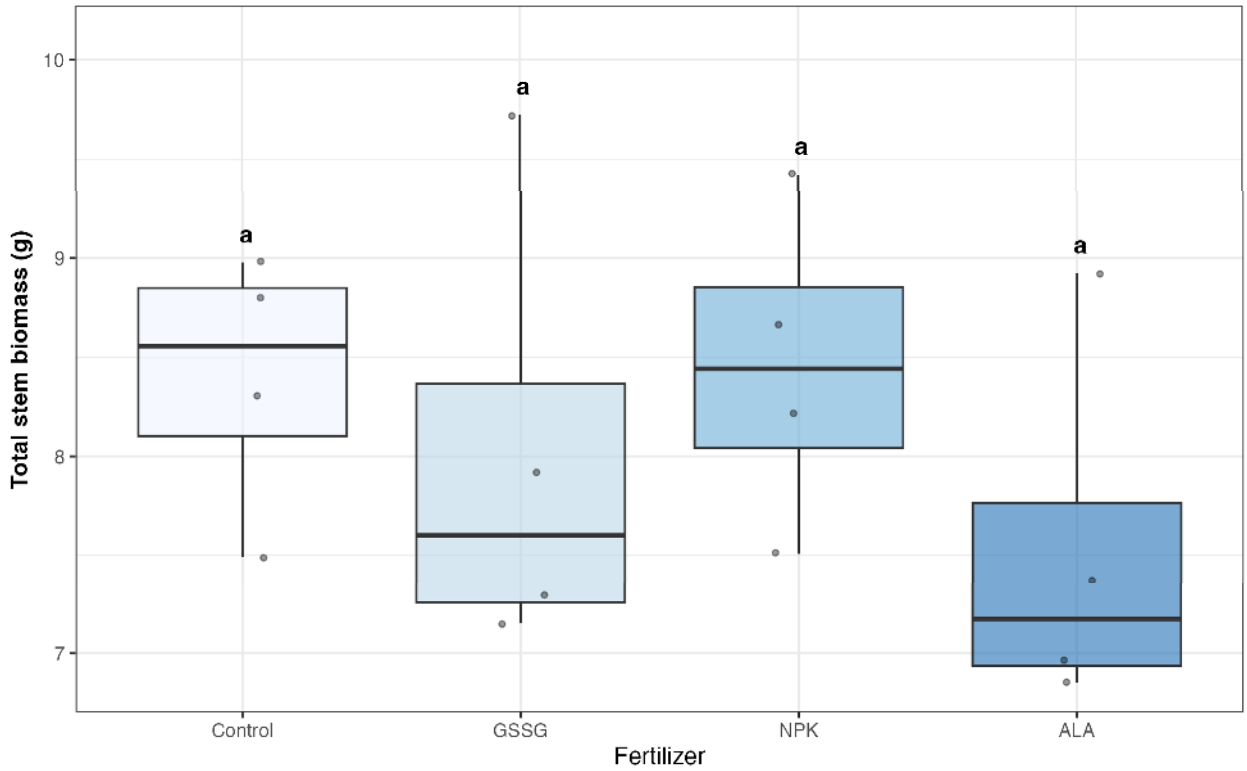

(**d**)

Figure 5. *Cont.*

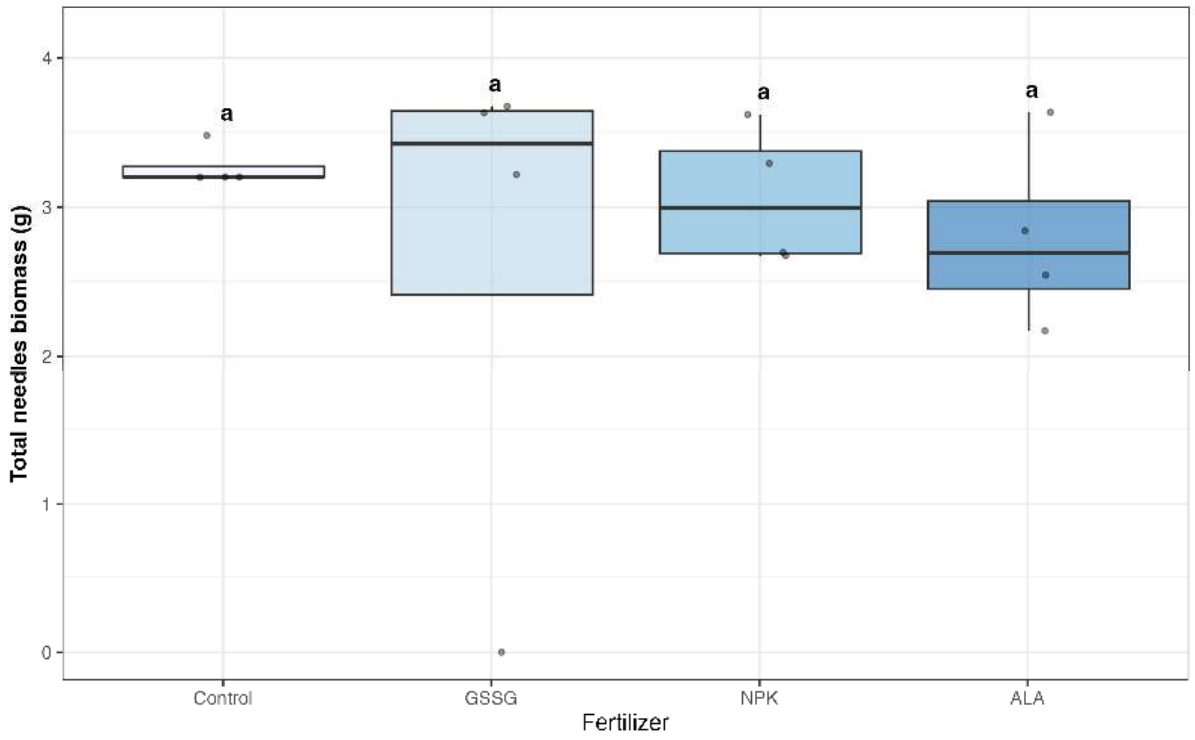

(**e**)

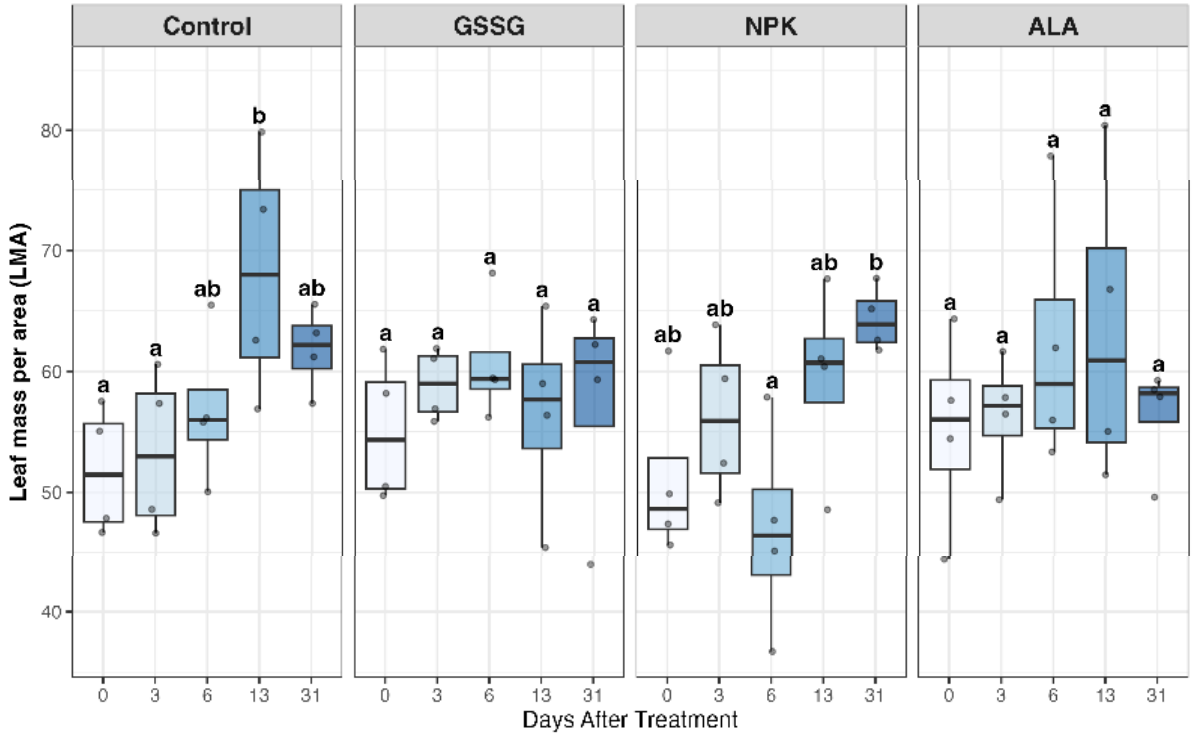

(**f**)

Figure 5. Graphical representation of the linear mixed-effects models for biomass traits. Comparisons among fertilizer treatments were performed for stem biomass within the terminal shoot in 2024 (**a**), needle biomass within the terminal shoot in 2024 (**b**), root biomass (**c**), total stem biomass (**d**), and total needle biomass (**e**). Pairwise contrasts between fertilizer treatment and observation time were performed separately for each fertilizer for leaf mass per area (LMA) (**f**). Different letters indicate significant differences among groups based on estimated marginal means, with *p*-values adjusted for multiple comparisons using Tukey's method ($p < 0.05$). Points represent the distribution of individual data points.

A similar numerical trend was observed for root biomass. The GSSG treatment yielded the highest numerical mean root dry weight and the largest estimated values among all treatments (Table 8). Analysis of the contrasts indicated that GSSG-treated saplings possessed numerically higher average root dry weights than the other groups, although these differences were not statistically significant (Figure 5c). The total stem and needle biomass (Figure 5d,e), as well as the biomass of needles within the terminal shoot in 2024 (Figure 5b), showed no significant variation across treatments. Furthermore, leaf mass per area (LMA), a key structural trait linking metabolic activity to biomass, was numerically higher in GSSG-treated saplings than in NPK-treated saplings (Figure 5f, Tables S20 and S31), although the linear mixed-effects model did not show any significant differences (Table S8).

4. Discussion

In this study, we evaluated the photosynthetic performance of *Larix gmelinii* var. *japonica* needles following foliar application of GSSG compared to ALA and NPK fertilizers. ALA is a small signaling molecule with various functions in plants, including enhancing antioxidant defense [36–39], similar to that of GSSG. A comparison of GSSG with ALA and common NPK fertilizers is expected to highlight its advantages over other antioxidative agents (ALA) and conventional NPK fertilizers. In addition to the weak effect of ALA in this study, the exact amount of ALA used in ALA-FeSTA remains unknown and is therefore considered insufficient for a detailed discussion.

To ensure leaf homogeneity and minimize the influence of leaf age on photosynthetic parameters, treatments were applied in early July 2024 to fully mature needles flushed in early March (Figure 1). This timing is critical because leaf age can significantly affect chlorophyll fluorescence and nutrient dynamics, as previously reported for various species [40,41]. Because all saplings exhibited uniform leaf maturation prior to treatment, the potentially confounding effects of leaf age were effectively excluded, allowing for a focused evaluation of the effects of the exogenous fertilizer treatments.

In this study, the timing of fertilizer application to three-year-old *L. gmelinii* var. *japonica* saplings aligned with the critical seedling stage of *Larix* and other conifers [5,15]. Enhancing photosynthetic performance at this stage is essential because it directly determines seedling production, post-planting growth, and survival in temperate species [1–3]. Exogenous glutathione is widely recognized for its ability to improve photosynthesis, primarily by acting as a non-enzymatic antioxidant that alleviates oxidative stress [21–25,28,29]. Recent studies have suggested that regulating glutathione metabolism can broadly optimize photosynthetic capacity under various conditions [26,27,42–45]. Consequently, the application of GSSG in the present study was expected to increase the photosynthetic resources available for robust sapling development and long-term growth.

4.1. Glutathione Accelerates Photosynthetic Rate Enhancement in Larix

The net CO_2 assimilation rate at light saturation (A_{max}) was used as an indicator of photosynthetic performance. Our results showed that GSSG application significantly increased A_{max} six days after treatment, representing the only group that exhibited a significant peak relative to Day 0 at this early stage (Figure 2a). This early increase in A_{max} may indicate a rapid physiological response to the GSSG treatment. However, as the underlying mechanisms were not directly examined in this study, the interpretation of this response should be made with caution. Previous studies have suggested that exogenous GSSG can be absorbed and converted into reduced glutathione (GSH), which is involved in redox regulation and cellular protection [46–48]. In addition, GSH has been reported to play a role in maintaining photosynthetic function under stress conditions [49–51]. Although

these findings provide a possible context for the observed response, further studies are required to clarify the mechanisms underlying the rapid enhancement of A_{max} observed in the present study.

4.2. Photosynthetic Responses to Light Conditions in Larix

Consistent with the A_{max} results, the GSSG treatment maintained F_v/F_m median values within the range typically associated with healthy, unstressed plants, indicating stable primary photochemical activity in photosystem II [52]. Although the intertreatment differences were not statistically significant, GSSG showed a slight upward trend between Days 3 and 13 ($p = 0.065$), which may indicate a transient response during this period. In addition, GSSG-treated saplings showed little change in F_v/F_m over time (-0.003, $p = 0.998$), suggesting that the F_v/F_m values remained close to baseline by Day 31 (Table 6). These results indicated that GSSG treatment did not negatively affect PSII efficiency during the experimental period.

While F_v/F_m represents the potential maximum efficiency of PSII, midday Φ_{PSII} reflects actual photosynthetic performance under high-light conditions. GSSG-treated saplings showed a different temporal pattern in Φ_{PSII} compared to the control, with a significant difference in the rate of change between groups ($\beta = 0.21$, $p = 0.019$) (Table 6, Figure 2c). However, the absolute differences between treatments were generally small. Overall, GSSG and other treatments showed less fluctuation in Φ_{PSII} measured at noon compared to the control, with values remaining closer to their Day 0 baseline by the end of the experiment (Table 9). These observations suggest differences in the response to midday light conditions, although the underlying mechanisms were not examined in this study. The early increase in A_{max} observed in GSSG-treated saplings may be associated with these patterns of PSII-related parameters. Previous studies have reported that glutathione is involved in maintaining photosynthetic function under stress conditions [29], which may provide a context for the observed responses. However, further investigations are required to clarify the relationships between these processes.

4.3. Carbon–Nitrogen Dynamics in Glutathione-Treated Larix

As a peptide-based fertilizer, GSSG has been reported to increase nitrogen (N) content in various plants [53,54]. Nitrogen is closely associated with photosynthetic functions, as leaf proteins account for a substantial proportion of foliar N [55–57]. In the present study, GSSG-treated saplings showed a significant increase in N content on Day 13 relative to the initial baseline, whereas the other treatments did not show such a pattern (Figure 3a). This temporal pattern may indicate differences in N dynamics among the treatments, although the underlying processes were not directly examined in this study. Previous studies have suggested that glutathione may require enzymatic processing before N becomes available for plant metabolism [58,59], which may provide a context for the observed pattern.

Carbon content remained relatively stable during the initial period but declined by Day 31 relative to the peak on Day 3 in GSSG-treated saplings (Figure 3b). As a result, the C:N ratio decreased significantly on Day 13, indicating a relative increase in N compared to carbon at this time point [60]. These patterns suggest temporal variations in carbon and nitrogen balance during the experimental period. Prior to the decline in the C:N ratio, the GSSG-treated saplings showed relatively stable values during the early stages. However, these patterns should be interpreted with caution, as the underlying physiological processes were not measured directly.

Regarding photosynthetic nitrogen use efficiency (PNUE), the peak in A_{max} observed at Day 6 occurred while leaf nitrogen remained at baseline levels (Figures 2a and 3a). Although this initially suggested a potential increase in efficiency, statistical analysis indicated that

PNUE was not significantly affected by the GSSG treatment (Figure 3d). These results suggest that the early increase in carbon assimilation was not accompanied by a detectable change in PNUE under the conditions used in this study.

Table 9. Linear mixed-effects model results for the effects of fertilizer treatment and observation time (Day) on carbon concentration. Carbon concentration was modeled with Fertilizer and Day as fixed factors and Plant_No as a random effect. *p*-values were calculated using Satterthwaite's method. The intercept represents the baseline group (Control Fertilizer at Day 0). Asterisks indicate significance: *** $p < 0.001$, * $p < 0.05$, . $p < 0.1$.

Term	Estimate (β)	Std. Error	df	*t* Value	*p* Value	Sig
Fixed effects						
(Intercept)	45.724604	0.362016	24.050563	126.305	<0.001	***
Fertilizer Main Effects						
Fertilizer (GSSG)	0.283445	0.511968	24.050563	0.554	0.5849	
Fertilizer (NPK)	−0.042749	0.511968	24.050563	−0.084	0.9341	
Fertilizer (ALA)	−0.190291	0.511968	24.050563	−0.372	0.7134	
Day Main Effects						
Day 3	0.348793	0.319191	48	1.093	0.28	
Day 6	−0.414776	0.319191	48	−1.299	0.2	
Day 13	−0.007742	0.319191	48	−0.024	0.9807	
Day 31	0.039849	0.319191	48	0.125	0.9012	
Interactions: Fertilizer × Day 3						
GSSG × Day 3	−0.014821	0.451404	48	−0.033	0.9739	
NPK × Day 3	0.436071	0.451404	48	0.966	0.3389	
ALA × Day 3	0.290871	0.451404	48	0.644	0.5224	
Interactions: Fertilizer × Day 6						
GSSG × Day 6	−0.338196	0.451404	48	−0.749	0.4574	
NPK × Day 6	0.306839	0.451404	48	0.68	0.4999	
ALA × Day 6	−0.017275	0.451404	48	−0.038	0.9696	
Interactions: Fertilizer × Day 13						
GSSG × Day 13	−0.213899	0.451404	48	−0.474	0.6378	
NPK × Day 13	−0.051463	0.451404	48	−0.114	0.9097	
ALA × Day 13	−0.060363	0.451404	48	−0.134	0.8942	
Interactions: Fertilizer × Day 31						
GSSG × Day 31	**−0.925532**	0.451404	48	−2.05	**0.0458**	*
NPK × Day 31	−0.80985	0.451404	48	−1.794	0.0791	.
ALA × Day 31	−0.891512	0.451404	48	−1.975	0.054	.
Random effects						
Groups Name	**Variance**	**Std. Dev.**				
Plant_No (Intercept)	0.3205	0.5661				
Residual	0.2038	0.4514				

4.4. Biomass Patterns in Glutathione-Treated Larix

Although the differences were not statistically significant, the GSSG-treated saplings showed higher root and stem biomass in the 2024 terminal shoot than the other treatments (Table 8). No clear differences in biomass allocation were detected among the organs. This pattern coincided with a significant decline in carbon percentage (Figure 3b) and an increase in nitrogen concentration on Day 13 (Figure 3a). Because these values are expressed as percentages, the decrease in carbon may reflect a relative dilution effect associated with changes in nitrogen content [61].

These observations may indicate a relationship between carbon–nitrogen dynamics and biomass patterns under GSSG treatment, although causal relationships cannot be determined based on the present data. Previous studies have reported that glutathione

application influences plant growth and development, including root-related traits [47]. Similar trends have been observed in other species, where glutathione treatment was associated with changes in photosynthetic traits and biomass [21,22,25,28]. However, the mechanisms underlying these responses remain unclear and require further investigation.

5. Conclusions

In conclusion, exogenous GSSG application resulted in an earlier peak in A_{max} in *Larix* saplings, which was associated with patterns observed in Φ_{PSII} and F_v/F_m. These findings are consistent with previous studies, suggesting that glutathione is involved in the regulation of photosynthetic responses under various conditions [21,23–27,62–65]. Although foliar N is essential for carbon fixation [55–57], previous studies have highlighted the role of glutathione in nitrogen metabolism under stress conditions [53,54]. In this study, under non-stress conditions, GSSG treatment was associated with an earlier increase in the photosynthetic rate, accompanied by temporal changes in carbon and nitrogen dynamics, rather than an increase in total nitrogen or biomass. Further studies are required to investigate the potential effects of GSSG under various environmental stress conditions. In addition, given the relatively small sample size, which may have contributed to the weak between-treatment differences, and the lack of direct mechanistic measurements in this study, future research should address these limitations using larger sample sizes and targeted physiological analyses.

Supplementary Materials: The following supporting information can be downloaded at: https://www.mdpi.com/article/10.3390/f17050530/s1.

Author Contributions: Conceptualization, Y.M., W.I., A.N., R.M. and H.K.; methodology, Y.M., N.H.M., W.I., A.N., R.M. and H.K.; software, Y.M., N.H.M. and R.S.R.; validation, Y.M., N.H.M., W.I., A.N., R.M. and H.K.; formal analysis, Y.M., N.H.M. and R.S.R.; investigation, Y.M., N.H.M. and R.S.R.; resources, W.I., A.N., R.M. and H.K.; data curation, Y.M., N.H.M. and R.S.R.; writing—original draft preparation, R.S.R.; writing—review and editing, R.S.R., Y.M., N.H.M., W.I., A.N., R.M. and H.K.; visualization, R.S.R., Y.M.; supervision, Y.M.; project administration, Y.M.; funding acquisition, Y.M., W.I., A.N., R.M. and H.K. All authors have read and agreed to the published version of the manuscript.

Funding: This research was funded by the Priority Research Funding of the Local Independent Administrative Agency, Hokkaido Research Organization, Hokkaido, Japan and Research Grant for Encouragement of PhD Students, Graduate School of Environmental, Life, Natural Science and Technology, Graduate School of Natural Science and Technology, and Graduate School of Environmental and Life Sciences, Okayama University.

Data Availability Statement: The data supporting the findings of this study are available from the corresponding author upon request.

Acknowledgments: We thank Fujio Hyodo (Okayama University, Japan) for his scientific guidance and support with nitrogen and carbon analyses during this study. We also thank the Division of Instrumental Analysis, Okayama University, for the nitrogen and carbon measurements.

Conflicts of Interest: The authors declare no conflicts of interest.

Abbreviations

The following abbreviations are used in this manuscript:

GSSG	Oxidized glutathione
ALA	5-aminolevulinic acid
A_{max}	Net CO_2 assimilation rate

Φ_{PSII}	Linear dichroism
F_v/F_m	Oxidized glutathione
v/v	Volume per volume
n	Number of replicates
NPK	Nitrogen, Phosphorus and Potassium
PSII	Photosystem II
F_o	The minimum fluorescence yield after dark adaptation under weak measurement light
F_m	The maximum fluorescence yield after dark adaptation under weak measurement light
F	Steady-state fluorescence under ambient light
F'_m	The maximum fluorescence during a saturating pulse
NPQ	Non-photochemical quenching
LMA	Leaf mass per area
PNUE	Photosynthetic nitrogen use efficiency
LMMs	Linear mixed-effects models
ANOVA	Analysis of variance
N	Nitrogen
C	Carbon
C:N	Carbon-to-nitrogen
GSH	Reduced glutathione
ATP	Adenosine triphosphate
df	Degrees of freedom
Std. Error	Standard error
Sig	Significance level

References

1. Oguchi, R.; Hiura, T.; Hikosaka, K. The Effect of Interspecific Variation in Photosynthetic Plasticity on 4-Year Growth Rate and 8-Year Survival of Understorey Tree Seedlings in Response to Gap Formations in a Cool-Temperate Deciduous Forest. *Tree Physiol.* **2017**, *37*, 1113–1127. [CrossRef]
2. Modrzyński, J.; Chmura, D.J.; Tjoelker, M.G. Seedling Growth and Biomass Allocation in Relation to Leaf Habit and Shade Tolerance among 10 Temperate Tree Species. *Tree Physiol.* **2015**, *35*, 879–893. [CrossRef]
3. Lee, B.R.; Ibáñez, I. Spring Phenological Escape Is Critical for the Survival of Temperate Tree Seedlings. *Funct. Ecol.* **2021**, *35*, 1848–1861. [CrossRef]
4. Peltier, D.M.P.; Ibanez, I. Patterns and Variability in Seedling Carbon Assimilation: Implications for Tree Recruitment under Climate Change. *Tree Physiol.* **2015**, *35*, 71–85. [CrossRef] [PubMed]
5. Kita, K.; Moriguchi, Y.; Kon, H. Breeding a hybrid larch in Hokkaido, northern Japan. *Eur. J. For. Res.* **2022**, *22*, 19–22. [CrossRef]
6. Harayama, H.; Tsuyama, I.; Uemura, A.; Kitao, M.; Han, Q.; Kuramoto, S.; Utsugi, H. Growth and Survival of Hybrid Larch F1 (*Larix gmelinii* Var. Japonica × *L. kaempferi*) and Japanese Larch under Various Intensities of Competition. *New For.* **2023**, *54*, 945–961. [CrossRef]
7. Annual Report on Forest and Forestry in Japan Fiscal Year 2024. Available online: https://www.rinya.maff.go.jp/j/kikaku/hakusyo/r6hakusyo/attach/pdf/zenbun-38.pdf (accessed on 11 March 2026).
8. Hokkaido Forestry Statistics Fiscal Year 2024. Available online: https://www.pref.hokkaido.lg.jp/sr/sum/kcs/rin-toukei/rin-toukei-index.html (accessed on 11 March 2026).
9. Jin, Y.; Li, J.; Bai, X.; Zhao, Y.; Cui, D.; Chen, Z. High Temperatures Constrain Latewood Formation in *Larix gmelinii* Xylem in Boreal Forests. *Glob. Ecol. Conserv.* **2021**, *30*, e01767. [CrossRef]
10. Zhao, X.; Hao, Y.; Wang, T.; Dong, L.; Li, F. Competition Is Critical to the Growth of *Larix gmelinii* and *Betula platyphylla* in Secondary Forests in Northeast China under Climate Change. *Glob. Ecol. Conserv.* **2024**, *51*, e02935. [CrossRef]
11. Du, H.; Xu, L.; Camarero, J.J.; Cherubini, P.; Li, M.-H.; He, H.S.; Meng, X.; Wu, Z. Radial Growth Responses of *Larix gmelinii* to Drought Events in Dry and Wet Areas of Northern Temperate Forests. *Dendrochronologia* **2024**, *84*, 126185. [CrossRef]
12. Zou, K.; Wang, J.; Lei, X.; Zhang, L.; Chen, D.; Yang, L.; Liu, X. Impacts of Climate and Competition on the Growth of *Larix Gmelinii* in Plantation: Implications for Forest Management in Temperate Regions. *Eur. J. For. Res.* **2026**, *145*, 27. [CrossRef]
13. Harayama, H.; Tobita, H.; Kitao, M.; Kon, H.; Ishizuka, W.; Kuromaru, M.; Kita, K. Enhanced Summer Planting Survival of Japanese Larch Container-Grown Seedlings. *Forests* **2021**, *12*, 1115. [CrossRef]

14. Harayama, H.; Tsuyama, I.; Kitao, M.; Yamada, T.; Furuya, N.; Utsugi, H.; Sasaki, S. Effects of Seedling Size, Stock Type, and Mechanical Site Preparation Method on Initial Survival and Growth of Japanese Larch (*Larix kaempferi*) Seedlings. *Forests* **2023**, *14*, 784. [CrossRef]
15. Owari, T.; Suzuki, S.N.; Tanaka, N.; Fukui, D. *Integrative Forest Management and Silviculture: Harmonizing Conservation and Production (Ecological Research Monographs)*; Springer Nature Singapore: Singapore, 2026. [CrossRef]
16. Kosinski, G. Empty Seed Production in European Larch (*Larix decidua*). *For. Ecol. Manag.* **1987**, *19*, 241–246. [CrossRef]
17. Slobodník, B. Pollination Success and Full Seed Percentage in European Larch (*Larix decidua* MILL.). *J. For. Sci.* **2002**, *48*, 271–280. [CrossRef]
18. Abaimov, A.P.; Barzut, V.M.; Berkutenko, A.N.; Buitink, J.; Martinsson, O.; Milyutin, L.I.; Polezhaev, A.; Putenikhin, V.P.; Takata, K. Seed collection and seed quality of Larix spp. from Russia: Initial phase on the Russian-Scandinavian Larch Project. *Eur. J. For. Res.* **2002**, *4*, 39–49.
19. Slobodník, B.; Guttenberger, H. Zygotic Embryogenesis and Empty Seed Formation in European Larch (*Larix decidua* Mill). *Ann. For. Sci.* **2005**, *62*, 129–134. [CrossRef]
20. Muhie, S.H. Optimization of Photosynthesis for Sustainable Crop Production. *CABI Agric. Biosci.* **2022**, *3*, 50. [CrossRef]
21. Suliman, M.S.E.; Elradi, S.B.M.; Zhou, G.; Meng, T.; Zhu, G.; Xu, Y.; Nimir, N.E.A.; Elsiddig, A.M.I.; Awdelseid, A.H.M.; Ali, A.Y.A.; et al. Exogenous Glutathione Protected Wheat Seedling from High Temperature and Water Deficit Damages. *Sci. Rep.* **2024**, *14*, 5304. [CrossRef]
22. Fan, J.H.; Jiang, Y.P.; Ren, X.N.; Shan, Y.; Li, X.; Li, Y.Y.; Wang, L.L.; Ma, L.J.; Li, X.M. Effect of Exogenous Glutathione on Photosystem II Functioning of Rice (*Oryza sativa* L.) Seedlings under Na_2CO_3 Stress. *Appl. Ecol. Environ. Res.* **2023**, *21*, 793–804. [CrossRef]
23. Cao, F.; Cai, Y.; Liu, L.; Zhang, M.; He, X.; Zhang, G.; Wu, F. Differences in photosynthesis, yield, and grain cadmium accumulation as affected by exogenous cadmium and glutathione in the two rice genotypes. *Plant Growth Regul.* **2015**, *75*, 715–723. [CrossRef]
24. Fatma, M.; Asgher, M.; Masood, A.; Khan, N.A. Excess Sulfur Supplementation Improves Photosynthesis and Growth in Mustard under Salt Stress through Increased Production of Glutathione. *Environ. Exp. Bot.* **2014**, *107*, 55–63. [CrossRef]
25. Ding, X.; Jiang, Y.; He, L.; Zhou, Q.; Yu, J.; Hui, D.; Huang, D. Exogenous Glutathione Improves High Root-Zone Temperature Tolerance by Modulating Photosynthesis, Antioxidant and Osmolytes Systems in Cucumber Seedlings. *Sci. Rep.* **2016**, *6*, 35424. [CrossRef]
26. Per, T.S.; Masood, A.; Khan, N.A. Nitric Oxide Improves S-Assimilation and GSH Production to Prevent Inhibitory Effects of Cadmium Stress on Photosynthesis in Mustard (*Brassica juncea* L.). *Nitric Oxide* **2017**, *68*, 111–124. [CrossRef]
27. Müller-Schüssele, S.J.; Wang, R.; Gütle, D.D.; Romer, J.; Rodriguez-Franco, M.; Scholz, M.; Buchert, F.; Lüth, V.M.; Kopriva, S.; Dörmann, P.; et al. Chloroplasts Require Glutathione Reductase to Balance Reactive Oxygen Species and Maintain Efficient Photosynthesis. *Plant J.* **2020**, *103*, 1140–1154. [CrossRef]
28. Abd El Mageed, T.A.; Semida, W.; Hemida, K.A.; Gyushi, M.A.H.; Rady, M.M.; Abdelkhalik, A.; Merah, O.; Brestic, M.; Mohamed, H.I.; El Sabagh, A.; et al. Glutathione-Mediated Changes in Productivity, Photosynthetic Efficiency, Osmolytes, and Antioxidant Capacity of Common Beans (*Phaseolus vulgaris*) Grown under Water Deficit. *PeerJ* **2023**, *11*, e15343. [CrossRef]
29. Cong, Y.; Chen, X.; Xing, J.; Li, X.; Pang, S.; Liu, H. Nitric Oxide Signal Is Required for Glutathione-Induced Enhancement of Photosynthesis in Salt-Stressed *Solanum lycopersicum* L. *Front. Plant Sci.* **2024**, *15*, 1413653. [CrossRef]
30. Professional Hyponex 20-20-20. Available online: https://www.hyponex.co.jp/products/prohypo202020/ (accessed on 6 March 2026).
31. Kaneka Fertiizer™/Kaneka Peptide®. Available online: https://kaneka-hokkaido.co.jp/business/fertilizer-peptide/ (accessed on 6 March 2026).
32. ALA-FeSTA (Ala Festa). Available online: https://www.sakataseed.co.jp/product/item/?code=30090601011 (accessed on 6 March 2026).
33. Schneider, C.A.; Rasband, W.S.; Eliceiri, K.W. NIH Image to ImageJ: 25 Years of Image Analysis. *Nat. Methods* **2012**, *9*, 671–675. [CrossRef]
34. Larcher, W. *Physiological Plant Ecology: Ecophysiology and Stress Physiology of Functional Groups*, 4th ed.; Springer Science & Business Media: Berlin/Heidelberg, Germany, 2003.
35. Posit team. *RStudio: Integrated Development Environment for R; Posit Software*; PBC: Boston, MA, USA, 2024. Available online: http://www.posit.co/ (accessed on 2 March 2024).
36. Wu, Y.; Liao, W.; Dawuda, M.M.; Hu, L.; Yu, J. 5-Aminolevulinic Acid (ALA) Biosynthetic and Metabolic Pathways and Its Role in Higher Plants: A Review. *Plant Growth Regul.* **2019**, *87*, 357–374. [CrossRef]
37. Ma, J.; Sun, M.; Qiu, L.; Xie, Y.; Ma, Y.; Liang, W. The 5-Aminolevulinic Acid (5-ALA) Supplement Enhances PSII Photochemical Activity and Antioxidant Activity in the Late Growth Promotion of *Pseudostellaria heterophylla*. *Plants* **2022**, *11*, 3035. [CrossRef] [PubMed]

38. Yang, L.; Wu, Y.; Wang, X.; Lv, J.; Tang, Z.; Hu, L.; Luo, S.; Wang, R.; Ali, B.; Yu, J. Physiological Mechanism of Exogenous 5-Aminolevulinic Acid Improved the Tolerance of Chinese Cabbage (*Brassica pekinensis* L.) to Cadmium Stress. *Front. Plant Sci.* **2022**, *13*, 845396. [CrossRef] [PubMed]
39. Wang, X.; Zhang, J.; Wang, L. Study on the Mechanism of Exogenous 5-Aminolevulinic Acid (ALA) in Regulating the Photosynthetic Efficiency of Pear Leaves. *Forests* **2024**, *15*, 769. [CrossRef]
40. Bielczynski, L.W.; Łącki, M.K.; Hoefnagels, I.; Gambin, A.; Croce, R. Leaf and Plant Age Affects Photosynthetic Performance and Photoprotective Capacity. *Plant Physiol.* **2017**, *175*, 1634–1648. [CrossRef]
41. Ji, M.; Jin, G.; Liu, Z. Effects of Ontogenetic Stage and Leaf Age on Leaf Functional Traits and the Relationships between Traits in *Pinus koraiensis*. *J. For. Res.* **2021**, *32*, 2459–2471. [CrossRef]
42. Nazar, R.; Umar, S.; Khan, N.A. Exogenous Salicylic Acid Improves Photosynthesis and Growth through Increase in Ascorbate-Glutathione Metabolism and S Assimilation in Mustard under Salt Stress. *Plant Signal. Behav.* **2015**, *10*, e1003751. [CrossRef]
43. Liu, W.; Zheng, C.; Chen, J.; Qiu, J.; Huang, Z.; Wang, Q.; Ye, Y. Cold Acclimation Improves Photosynthesis by Regulating the Ascorbate–Glutathione Cycle in Chloroplasts of *Kandelia obovata*. *J. For. Res.* **2019**, *30*, 755–765. [CrossRef]
44. Zhang, G.; Ba, Q.; Chen, S.; Liu, F.; Li, G. Exogenous Application of Glycine Betaine Alleviates Cadmium Toxicity in Super Black Waxy Maize by Improving Photosynthesis, the Antioxidant System and Glutathione-Ascorbic Acid Cycle Metabolites. *CEREAL Res. Commun.* **2020**, *48*, 449–458. [CrossRef]
45. Shad, M.I.; Ashraf, M.A.; Rasheed, R.; Hussain, I.; Ali, S. Exogenous Coumarin Decreases Phytotoxic Effects of Manganese by Regulating Ascorbate–Glutathione Cycle and Glyoxalase System to Improve Photosynthesis and Nutrient Acquisition in Sesame (*Sesamum indicum* L.). *J. Soil. Sci. Plant Nutr.* **2023**, *23*, 251–274. [CrossRef]
46. Rai, G.K.; Kumar, P.; Choudhary, S.M.; Singh, H.; Adab, K.; Kosser, R.; Magotra, I.; Kumar, R.R.; Singh, M.; Sharma, R.; et al. Antioxidant Potential of Glutathione and Crosstalk with Phytohormones in Enhancing Abiotic Stress Tolerance in Crop Plants. *Plants* **2023**, *12*, 1133. [CrossRef]
47. Mohri, T.; Uekita, K.; Saito, H.; Shiraiwa, T.; Nojiri, M. Exogenous Application of Oxidized Glutathione During the Seedling Stage Promotes Root Growth After Transplantation and Potentially Increases Panicles in Rice. *Int. J. Agron.* **2024**, *2024*, 1884599. [CrossRef]
48. Foyer, C.H.; Noctor, G. Ascorbate and Glutathione: The Heart of the Redox Hub. *Plant Physiol.* **2011**, *155*, 2–18. [CrossRef] [PubMed]
49. Nahar, K.; Hasanuzzaman, M.; Alam, M.D.M.; Fujita, M. Glutathione-Induced Drought Stress Tolerance in Mung Bean: Coordinated Roles of the Antioxidant Defence and Methylglyoxal Detoxification Systems. *AoB Plants* **2015**, *7*, plv069. [CrossRef]
50. Nahar, K.; Hasanuzzaman, M.; Alam, M.M.; Fujita, M. Roles of exogenous glutathione in antioxidant defense system and methylglyoxal detoxification during salt stress in mung bean. *Biol. Plant* **2015**, *59*, 745–756. [CrossRef]
51. Nahar, K.; Hasanuzzaman, M.; Suzuki, T.; Fujita, M. Polyamines-Induced Aluminum Tolerance in Mung Bean: A Study on Antioxidant Defense and Methylglyoxal Detoxification Systems. *Ecotoxicology* **2017**, *26*, 58–73. [CrossRef]
52. Arief, M.A.A.; Kim, H.; Kurniawan, H.; Nugroho, A.P.; Kim, T.; Cho, B.-K. Chlorophyll Fluorescence Imaging for Early Detection of Drought and Heat Stress in Strawberry Plants. *Plants* **2023**, *12*, 1387. [CrossRef]
53. Zhang, L.; Suo, L.; Shan, Y.; Wang, B. Glutathione Alleviates Boron Toxicity by Modulating Nitrogen Metabolism and Boronuptake in Rice Seedlings. *Turk. J. Agric. For.* **2024**, *48*, 1011–1022. [CrossRef]
54. Riaz, M.; Hussain, S.; Ali, Q.; Yan, L. Glutathione Promotes Aluminum Tolerance in Rice through Cell Wall Remodeling and Nitrogen Metabolic Regulation. *Ecotoxicol. Environ. Saf.* **2025**, *302*, 118561. [CrossRef]
55. Bassi, D.; Menossi, M.; Mattiello, L. Nitrogen Supply Influences Photosynthesis Establishment along the Sugarcane Leaf. *Sci. Rep.* **2018**, *8*, 2327. [CrossRef]
56. Mu, X.; Chen, Y. The Physiological Response of Photosynthesis to Nitrogen Deficiency. *Plant Physiol. Biochem.* **2021**, *158*, 76–82. [CrossRef]
57. Noor, H.; Ding, P.; Ren, A.; Sun, M.; Gao, Z. Effects of Nitrogen Fertilizer on Photosynthetic Characteristics and Yield. *Agronomy* **2023**, *13*, 1550. [CrossRef]
58. Ito, T.; Kitaiwa, T.; Nishizono, K.; Umahashi, M.; Miyaji, S.; Agake, S.; Kuwahara, K.; Yokoyama, T.; Fushinobu, S.; Maruyama-Nakashita, A.; et al. Glutathione Degradation Activity of Γ-GLUTAMYL Peptidase 1 Manifests Its Dual Roles in Primary and Secondary Sulfur Metabolism in Arabidopsis. *Plant J.* **2022**, *111*, 1626–1642. [CrossRef]
59. Miyaji, S.; Ito, T.; Kitaiwa, T.; Nishizono, K.; Agake, S.; Harata, H.; Aoyama, H.; Umahashi, M.; Sato, M.; Inaba, J.; et al. N2 -Acetylornithine Deacetylase Functions as a CYS-GLY Dipeptidase in the Cytosolic Glutathione Degradation Pathway in *Arabidopsis thaliana*. *Plant J.* **2024**, *118*, 1603–1618. [CrossRef] [PubMed]
60. Zheng, Z.-L. Carbon and Nitrogen Nutrient Balance Signaling in Plants. *Plant Signal. Behav.* **2009**, *4*, 584–591. [CrossRef]
61. Kaspari, M.; Welti, E.A.R. Nutrient Dilution and the Future of Herbivore Populations. *Trends Ecol. Evol.* **2024**, *39*, 809–820. [CrossRef]

62. Noctor, G.; Mhamdi, A.; Chaouch, S.; Han, Y.; Neukermans, J.; Marquez-Garcia, B.; Queval, G.; Foyer, C.H. Glutathione in Plants: An Integrated Overview. *Plant Cell Environ.* **2012**, *35*, 454–484. [CrossRef]
63. Jefferies, H.; Coster, J.; Khalil, A.; Bot, J.; McCauley, R.D.; Hall, J.C. Glutathione. *ANZ J. Surg.* **2003**, *73*, 517–522. [CrossRef] [PubMed]
64. Rouhier, N.; Lemaire, S.D.; Jacquot, J.-P. The Role of Glutathione in Photosynthetic Organisms: Emerging Functions for Glutaredoxins and Glutathionylation. *Annu. Rev. Plant Biol.* **2008**, *59*, 143–166. [CrossRef] [PubMed]
65. Ding, S.; Ma, C.; Shi, W.; Liu, W.; Lu, Y.; Liu, Q.; Luo, Z.-B. Exogenous Glutathione Enhances Cadmium Accumulation and Alleviates Its Toxicity in *Populus* × *canescens*. *Tree Physiol.* **2017**, *37*, 1697–1712. [CrossRef] [PubMed]

Disclaimer/Publisher's Note: The statements, opinions and data contained in all publications are solely those of the individual author(s) and contributor(s) and not of MDPI and/or the editor(s). MDPI and/or the editor(s) disclaim responsibility for any injury to people or property resulting from any ideas, methods, instructions or products referred to in the content.